Boulder Atmosphere Innovation Research

Boulder A.I.R. L.L.C; 2820 Lafayette Dr., Boulder, CO 80305, U.S.A.; dh.bouldair@gmail.com

November 16, 2020

To:

City of Longmont
350 Kimbark Street
Longmont, CO 80501

Attn: Dr. Jane Turner

Re: Longmont Regional Air Quality Study – Year 2020 Quarter 1 Report

Dear Dr. Turner,

Please find included with this letter the revised January – March (Quarter 1) 2020 report for our work on the Longmont Air Quality Study. This report describes the completion of the monitoring equipment installation. In addition, the 2020 Quarter 1 monitoring data and selected analyses are presented.

Thank you for providing this opportunity for air quality monitoring to Longmont citizens and the City of Longmont. We would be happy to discuss any questions that you, other City staff or Longmont citizens may have.

Sincerely,

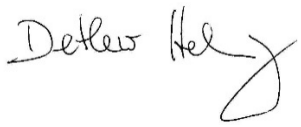

Detlev Helmig

Boulder AIR LLC

2020 Quarter 1 (January – March) Report

Longmont Air Quality Study

Executive Summary

This report summarizes the completion of the monitoring equipment installation for the Longmont Air Quality Study and data collection during January through March of 2020. The Longmont Municipal Airport (LMA) site became fully operational in September 2019. The installation of the monitoring shelter at the Longmont Union Reservoir (LUR) was completed in early December 2019. The first instruments were installed and became operational at LUR during mid-December 2019. The installation continued during January 2020 with the meteorological data system, and instruments for measuring particulate matter (PM) and volatile organic compounds (VOCs). All variables, except VOCs, were included in the real-time reporting on the public *Longmont Air Quality Now* website by the end of January. The reporting of VOCs on the web portal became fully functional by mid-March 2020.

This report includes graphical analyses of all data acquired during January-March, 2020. In addition, data comparisons and analyses of selected events that resulted in enhanced concentrations are presented. LMA and LUR data are compared with each other and also with concurrent observations from the Boulder Reservoir. Differences between the two sites are most notable for methane and VOCs, where average concentrations at LUR are higher than at LMA. In addition, a higher frequency of elevated concentration spikes was observed at LUR. A preliminary transport analysis, based on associated wind direction during observed peak concentrations, suggests that the source of these pollutants is predominantly from the northwest to northeast of LUR.

Table of Contents

1. Project Overview

The scope of the Longmont air monitoring project has been covered in the "2019 Summary Report - Longmont Air Quality Study" and only a few details are summarized here. Boulder A.I.R. provides continuous ambient monitoring of gaseous pollutants, greenhouse gases, meteorological variables and particle mass concentrations. The list of variables include:

- Ozone (O_3)
- Meteorological variables (Temperature, relative humidity, solar radiation, wind speed and direction)
- CO_2
- NO_x ($NO + NO_2$)
- Methane (CH_4)
- Volatile Organic Compounds (VOCs)
- Particulate matter mass ($PM_{2.5}$, PM_{10})
- Webcam for showing visible site conditions (snow, light, vegetation)

Additional details are provided below. All of these atmospheric constituents influence air quality and provide data on emissions, transport, and spatial variability. Measurements are taken at two locations within the boundaries of the City of Longmont – Union Reservoir and Longmont Municipal Airport. Data are uploaded to public websites where the concentrations measured over the last 3 or 30 days can be viewed within minutes of the latest observations. Data analyses and interpretations are provided to the City of Longmont in public presentations, and quarterly, and annual reports. Numerical data will be shared upon request through a data sharing agreement after the data are quality checked.

2. Air Quality Monitoring Study Updates

The installation of all monitoring equipment at LMA was completed in September 2019 and data collection has continued throughout Quarter 1 2020. Installations at LUR began once power and internet became available on December 12, 2019. The instruments for monitoring ozone, CO_2, methane, and nitrogen oxides became operational in December. The installation was fully competed in January when the data acquisition for the meteorological instruments, particulate matter monitor, and VOCs instrument started sampling. The timeline summarizing the years 2019-2020 progress is provided in Table 1.

The following major equipment items were installed at LUR:

- Picarro-G2401 methane/CO_2 analyzer
- One GRIMM EDM-180 particles ($PM_{2.5}$ and PM_{10}) analyzer
- Thermo Environmental Model 49C UV absorption ozone monitor
- Thermo Environmental Model 49C PS ozone calibrator
- Teledyne API-T200P ultratrace nitrogen oxides monitor with photolytic NO_2 converter
- Meteorological sensors
    - wind speed/direction (RM Young Wind Monitor AQ)
    - temperature/humidity sensor (CSL Temperature/RG Probe) in radiation shield
    - visible spectrum radiation sensor (Apogee SP-110-SS)
- Webcam (Amcrest UltaHD 4K)
- Campbell CRX data logger (CR1000X)
- Data system computer

- Thermo Environmental Model 146i calibrator for nitrogen oxides calibration
- Two Synaccess Netbooters for remote systems startup/shut down
- One custom-built pre-concentration system for VOCs, interfaced to an Agilent 5890 gas chromatograph with flame ionization detector
- SRI gas chromatography data system (SRI single channel model 333)
- One nitric oxide primary calibration standard (Praxair, 1 ppm – balance nitrogen)
- Two VOCs primary calibration standards (National Physics Laboratory, U.K.)
- Two primary methane and CO_2 calibration standards from the NOAA Global Monitoring Laboratory, Boulder

A picture showing the completed LUR instrument installation is provided in Figure 1.

3. Data Quality Insurance and Quality Control

The data quality protocols were previously reported in the 2019 report. A general summary along with few specifics are provided below. Data from the monitors are recorded to the instruments' computers at different intervals (depending on the measurement). Every 10 minutes, all data are backed up to a central server. Data processing occurs to convert raw signals into concentrations. These concentrations and webcam images are subsequently posted to the website approximately once every 10 minutes.

To ensure that the measurements are accurate, instruments are routinely calibrated with certified standards as indicated below.

1. Nitrogen Oxides: A 1-ppm NO standard from Praxair is used. This standard is diluted with scrubbed ambient air (Sofnofil and charcoal) using the Thermo Environmental 146i dynamic dilution calibrator. A zero and 2 span checks (40 ppb and 160 ppb) are run every two weeks. The NO_2 converter efficiency is tested with the 146i as well, by converting a fraction of the NO to NO_2, and then tracing the total NO_x result.

2. VOCs are calibrated using a certified multicomponent 10-ppb standard that was acquired from the U.K. National Physics Laboratory – the central calibration laboratory used for VOCs by the World Meteorological Organization (https://www.npl.co.uk/products-services/gas/volatile-organic-compounds-vocs). This standard is run weekly during site visits. In addition, a 200-ppb NPL standard is run quarterly to check for the linearity of the instrument response. A zero air (blank) sample and a Boulder A.I.R. laboratory-prepared multi-component working standard are run every 65 runs (every ~three days).

3. The $PM_{2.5}$ and PM_{10} measurements use the Grimm factory-provided calibration variables. Bi-weekly instrument maintenance includes checks of sample flow, humidity and temperature. The analyzer is certified by the United States EPA as a federal equivalent method for particulate mass concentration (see https://www.grimm-aerosol.com/products-en/environmental-dust-monitoring/approved-pm-monitor/edm180-the-proven/). Calibration is verified by the manufacturer after 1.5 years use.

4. Factory calibration functions are used for all meteorological measurements. The wind direction was calibrated by orienting anemometer to the north direction according to the instrument instructions. The accuracy of the wind direction orientation is estimated to be ± 15 degrees.

4. Website Development

A web portal, named *Longmont Air Quality Now*, was developed that reports the monitoring data from both sites in near real time to the public. Data from different instruments were added sequentially to the website as they became available. The final data added to the website were the speciated VOCs from LUR, which occurred on March 20, 2020. Three independent computers are used to back up data from each of the instruments' computers on an hourly basis. Examples of data from different instruments reported to the website are included below. Other details regarding the website development were reported in the 2019 annual report.

5. Data for Quarter 1, 2020

The data that were recorded in Q1 2020 are included in this report in graphical time series format as Supplement A (LMA) and Supplement B (LUR). These graphs provide the records of the completeness of the data coverage and general features in the dynamic, diurnal, and seasonal changes in the data. Some of the data (e.g. wind direction) are difficult to interpret when 3 months of data are included in the same plot. In these instances, the primary objective is to show general trends and that the data is nearly continuous – not to point out individual features. Data coverage for all variables is >95% for all periods shown in Table 1 (dark green colors). In Supplement C, the variables that are measured at both sites are shown together in a set of time series graphs. These graphs are presented to highlight similarities and differences between the two locations. The interactive data tool (IDAT) developed by Boulder A.I.R. is available for any user to observe each of the variables collected from any of the sites with a user-specified time window (http://www.bouldairtools.com/interactive/).

6. Selected Data Examples and Preliminary Interpretations

Please note that all data analyses and interpretations presented in this section are based on preliminary data and analyses. Further data quality control and analyses will need to be completed before final conclusions can be drawn.

Ozone

The winter-spring season is the time of year when there is relatively little local/regional ozone production and observed levels of ozone are mostly determined by the large-scale ozone background. The ozone records (Figure SA8 for LMA, Figure SB8 for LUR) show that for both sites ozone oscillated between <1 to ~50 ppb during most times. These levels are well below the 70 ppb ozone NAAQS, as can be seen in Figures SA9 and SB9, where the ozone data are averaged to an 8-hour running mean for comparison with the National Ambient Air Quality Standard (NAAQS) that is indicated by the yellow dotted line in these graphs.

The comparison of the monthly data distribution (Figure 2), also including the data from the Boulder Reservoir (BRZ), shows that BRZ has the overall higher ozone values, followed by LMA, and LUR. These relatively lower values at LMA and LUR are mostly determined by the higher abundance of low concentration values. This is a typical winter phenomenon. Figure 3 shows as an example a one-week ozone data window overlaying the LMA and LUR observations. While daytime values are similar at both sites, nighttime minima drop to lower, and to longer sustained lower values at LUR. This behavior is an indication of a stronger loss of ozone from a higher rate of destruction of ozone at LUR during the night, which most likely is driven by higher levels of nitric oxide at LUR, as NO is a primary ozone sink in the absence of light due to the reaction $NO + O_3 \rightarrow NO_2 + O_2$.

CO_2

Carbon dioxide levels behave the opposite to ozone with higher nighttime levels at LUR compared to LMA (Figure 4). This is likely due to overall stronger sources of CO_2 surrounding the site, or possibly to a stronger nocturnal boundary layer that promotes the accumulation of CO_2 near the surface at night. This nighttime behavior has a strong influence on the overall distribution of CO_2. As shown in the statistical analysis of the data in Figure 5, the lower end of the values are very similar, whereas the higher end distribution values show a wider spread and overall higher values at LUR. The concentration wind rose and heat map analyses (Figure 6, 7) show that for LMA the dominant CO_2 source region is the area to the east of the station, i.e. the City of Longmont, whereas for LUR, the predominant source region is to the west (City of Longmont) with other notable contributions to the north of the site.

Methane

There is a stark difference in methane between the two sites. Methane levels are LUR are more variable, and concentration peaks reach significantly higher levels compared to LMA (Figure 8). In between those concentration spikes there are periods when both stations measure similar levels. Those conditions are predominately characterized by strong, westerly winds, when air is quickly mixed and exchanged within the City footprint. It is striking that many of the methane peaks are of relatively short duration, i.e. on the order of a few minutes to a quarter hour. Figure 9 shows an enlargement of one of these methane events. Observed on March 26, this was the highest methane occurrence during Q1, with methane peaking at 32 ppm. This is a significant methane enhancement. For comparison, in three years of methane monitoring at the Boulder Reservoir, three has not been a single measurement exceeding the 5 ppm threshold.

Figure 10 provides an analysis of the transport conditions during the event by overlaying the occurrence of the methane spike with wind recordings of wind direction of wind speed. According to this analysis, during the 14-min window of the methane peak, winds were from the northwest (335 degrees) and at a relatively moderate wind speed of ~2.1 m/s.

Figure 11 places those variables on a site map, with an arrow added that indicates the direction of the air transport. The dotted lines define the estimated error bounds of the wind direction measurement. Please be aware that these error bounds do not necessarily reflect the uncertainty in the actual air travel path as winds monitored on the tower next to the station may be influenced by flow distortion at the site, such as by the building structure and nearby trees. Also, there is no certainty in how far the wind direction measured at the site extended along that same direction path upwind of the station. Wind data from other nearby weather stations could possibly be considered for assessing the magnitude of this uncertainty, though it will likely also depend on the wind speed. Therefore, caution should be exercised in the interpretation of the wind analysis and association of potential emissions sources that align with this wind vector analysis.

Figures 6 and 7 show the results of the methane wind dependency analysis for the full data set. In these results, the occasional and relatively short duration concentration spikes exert a relatively minor influence. Nonetheless, this analysis confirms the example that was discussed above: For LUR, on average, methane concentration enhancements are mostly associated with transport from the north to east sector. For LMA, methane sources are located in a wider sector, stretching from north to south, with a maximum straight to the east.

In Figure 12, all Q1 data are summarized in box whisker plots, including BRZ. In this comparison, during each of the Q1 months, the methane distribution is highest at LUR for all percentile levels, followed by LMA, and BRZ.

VOCs

Monitoring data for VOCs became available at the beginning of February. Overall, some 20 VOCs are monitored. This report focuses on a few select species to illustrate the general VOC behavior. The full records of available data are given in Figures SB10 to SB16. The abundance and the high levels observed in VOCs are quite remarkable. The general features of these spikes were similar as for methane, i.e. concentration spikes were relatively short in duration, and occurred irregularly. Ethane and propane are primary oil and gas tracer compounds. Their peak levels exceeded 500 ppb, and there were on the order of 20-40 occurrences during Q1 when their mole fractions exceeded 100 ppb. This compares to one single event at BRZ when ethane exceeded the 100 ppb threshold over the now 3+ years of monitoring at that site. In Figure 13, ~10 days of data from BRZ and LUR are overlaid. While there are periods when both sites report similar levels at the lower end of the data distribution, reflecting the regional background, a much higher frequency of concentration spikes, and higher resulting spikes concentrations, are seen at LUR.

The VOC sampling occurs during a 10 minute pre-concentration interval, so these data only reflect a fraction of the overall time window. It is therefore likely that there were more spikes, but that those may have been missed because sampling did not occur during that window. That was, for instance, the case for the methane spike discussed above. The 14 minutes of the methane spike did not coincide with the sampling interval for the VOC collections, so there are no VOCs data that overlap with this methane spike. In order to increase the chances to capture these frequent and short spikes, the sampling frequency was progressively increased from the 2-hour interval to ~hourly during February-March.

Similar behavior was seen for other VOCs, including propane, the butane isomers, and pentane isomers. This report focuses on one further VOC, i.e. benzene, motivated by the high interest of this VOC due to its recognized health effects as a carcinogen. Figure 14 shows the overlay of BRZ and LUR benzene for the full Q1 record, and a 10-day window of the data at higher resolution. There are far more spikes in benzene at LUR than at BRZ, and these spikes reach overall higher levels. There were many occurrences of benzene within the 1-10 ppb mole fraction range, while at BRZ, benzene always remained well below 1 ppb.

Figure 15 presents a similar wind transport analysis as shown above for methane. This particular example is for the highest benzene peak that was observed during Q1, i.e. at 8.6 ppb on February 20, at 19:04 hours. This benzene occurrence coincided with a peak in methane, as can be seen in the higher time resolution methane graph. Winds during the sampling interval were from the northwest sector, similar to the methane peak analysis presented above. The clear association/correlation of the benzene peak with methane suggests either a co-location of sources, or a shared source of methane and benzene.

In Figure 16, this analysis is taken further, now considering the ten highest benzene occurrences in Q1. There is a consistent behavior, as all of these high benzene occurrences appear to be associated with northwest to northeasterly winds. Please note again the limitations on the accuracy of using a single point wind observation for this type of analysis, as already explained above in the methane section. Nonetheless, this analysis suggests that there is a primary source for elevated benzene located to the north of LUR.

Figure 17 presents the statistical comparison of observed mole fractions of three selected VOCs between BRZ and LUR for the full Q1 record. As already evident and discussed for the case studies, VOC levels at LUR are higher throughout all months and at all percentile values in comparison to BRZ.

Tables and Figures

Table 1
Year 2019-2020 Longmont air monitoring sites installation and operation log. Light green colored periods indicate a process in progress, and dark green colored periods indicate a completed task or an operation that is meeting the final objectives.

	2019				
Activity	**March-August**	**September**	**October**	**November**	**December**
Site selection, visits, website design Instrument shelter design/specifications Building/instrument acquisitions					
LMA building in place with power LMA monitoring operation LMA data reporting on website					
LUR building in place with power LUR monitoring operation LUR data reporting on website					

	2020		
Activity	**January**	**February**	**March**
LMA monitoring operation LMA data reporting on website			
LUR monitoring operation LUR data reporting on website			

Roof Inlet for Particle Sampling

Tower with Gas Sampling Inlets, Meteorological Sensors, Webcam

Instruments for
- Ozone
- Nitrogen Oxides
- VOCs
- Methane
- CO_2
- Communication
- Automated Calibration
- Data Logging
- Calibration Gases

GRIMM EDM-180 Particle Monitor; PM2.5, PM10

Figure 1: Photographs of completed installation at LUR. Clockwise from top left are the particle inlet on top of the trailer, meteorological tower with sampling inlets, and instruments for gas-phase and particle monitoring located inside the trailer.

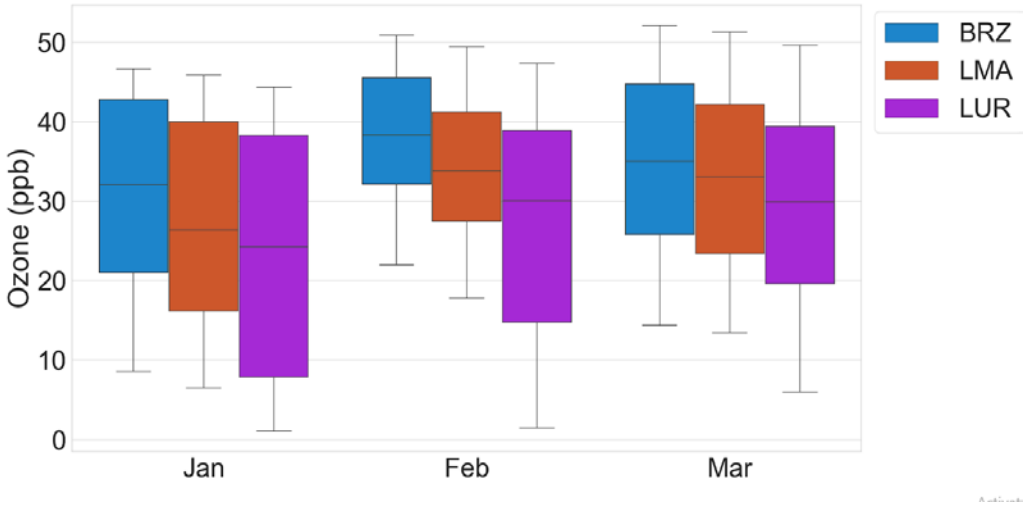

Figure 2:
Comparison of the ozone distribution at the Boulder Reservoir (BRZ), Longmont Municipal Airport (LMA), and Longmont Union Reservoir (LUR) during January – March 2020. These (and following) box whisker plots show the median value as the center line, the 25-75 percentile distribution as the colored boxes, and the 5-percentile and 95-percentile values as the whiskers.

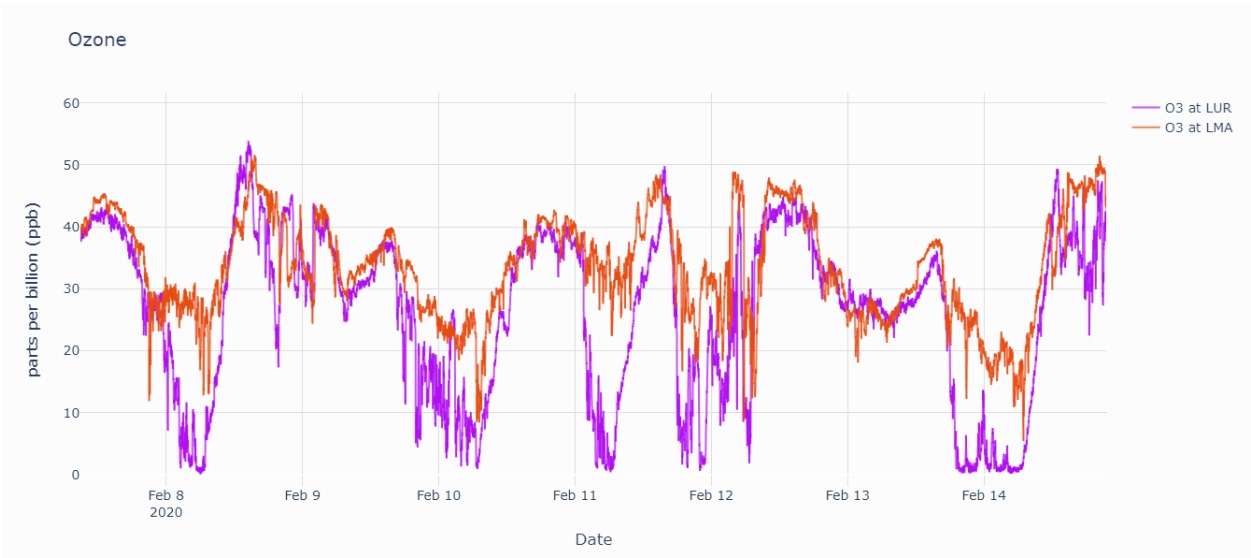

Figure 3:
Comparison of ozone recordings from LMA and LUR during one week in February.

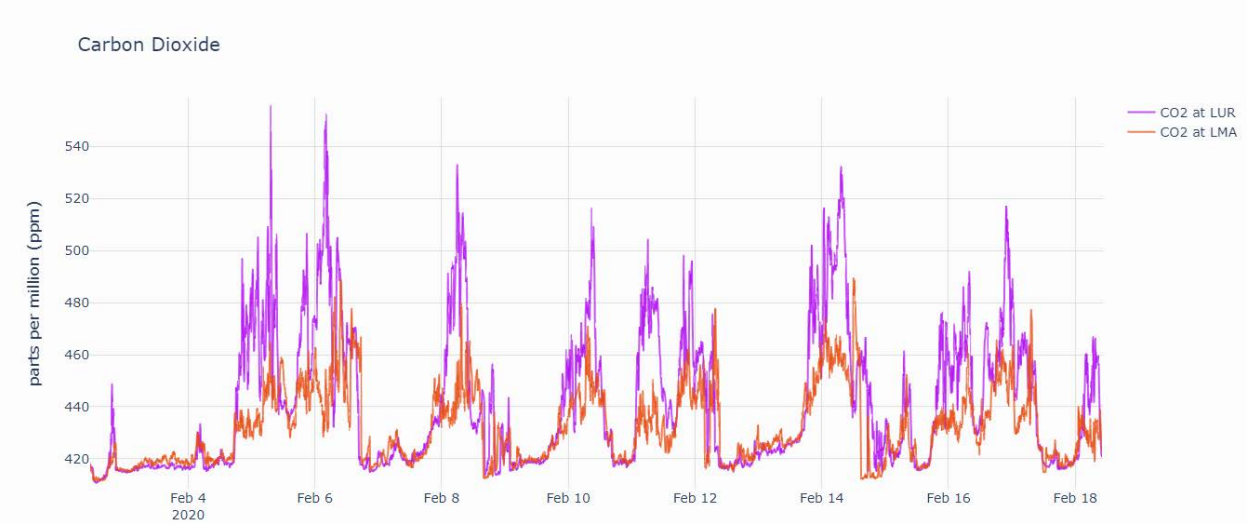

Figure 4:
Comparison of CO_2 at LMA and LUR during one week in February 2020.

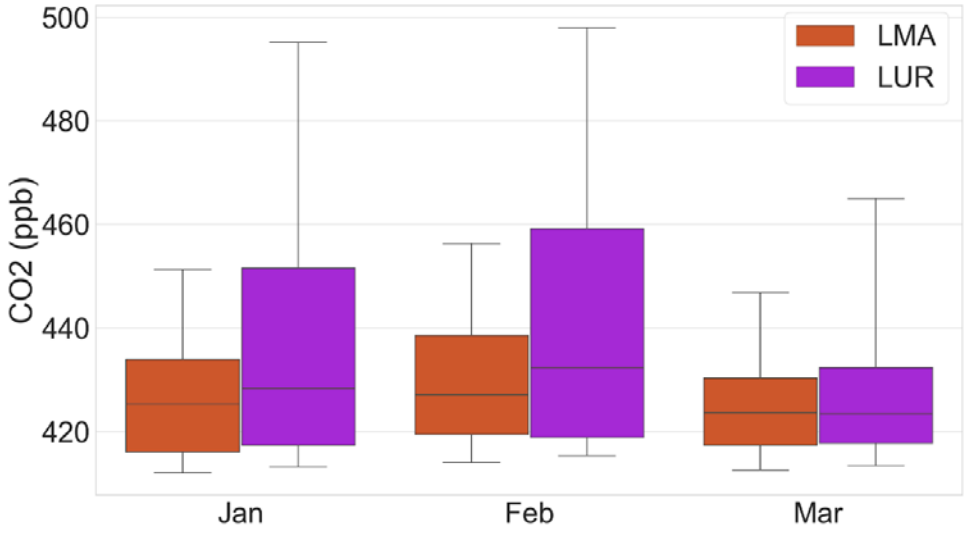

Figure 5:
Comparison of the CO_2 distribution at LMA, and LUR during January – March 2020. See Figure 2 for explanation of the box whisker plot formats.

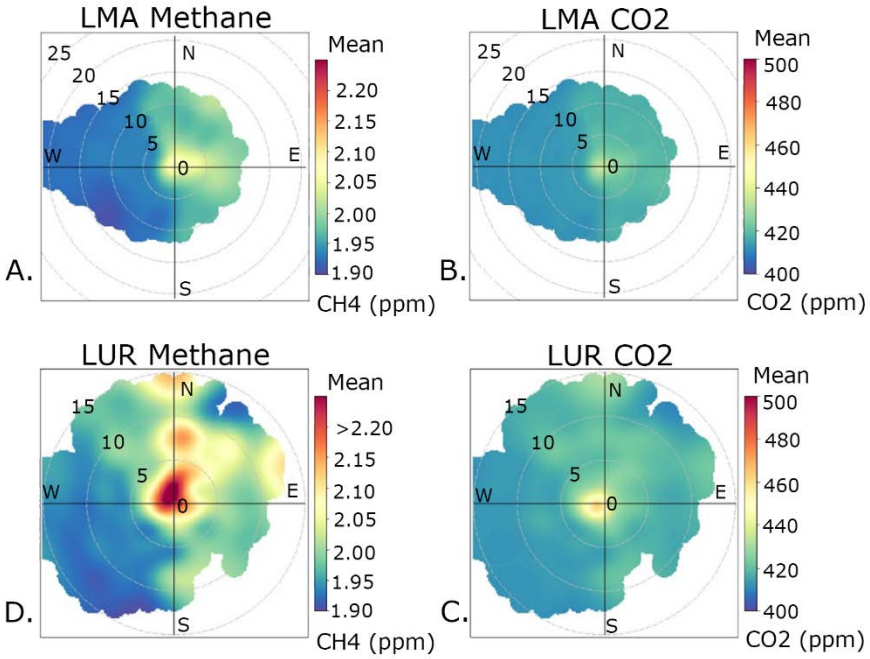

Figure 6:
Analysis of methane (left) and CO_2 (right) observed at LMA (top) and LUR (bottom) as a function of wind speed and wind direction.

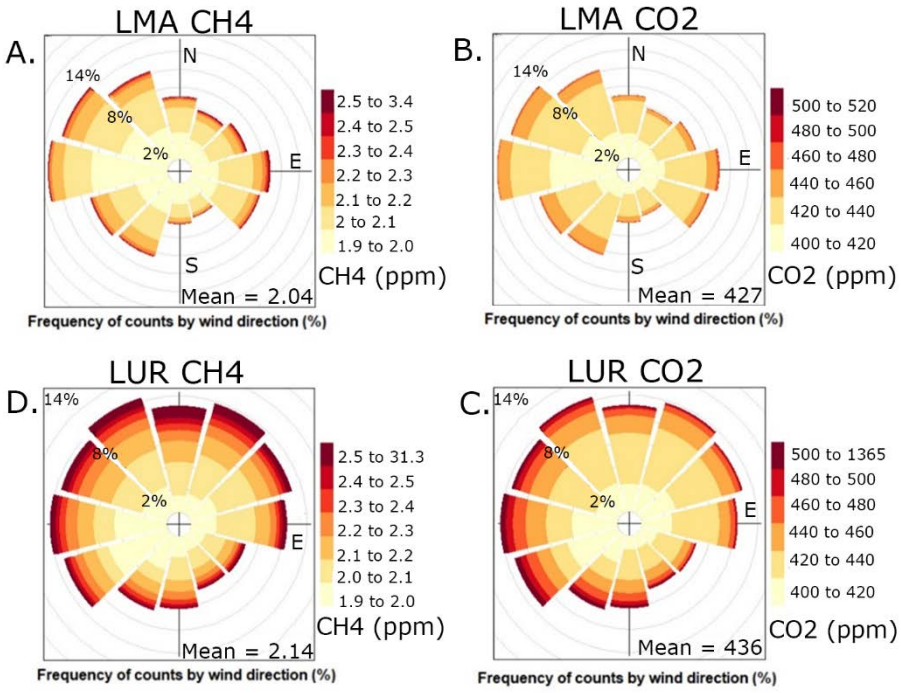

Figure 7:
Similar to Figure 6, but with observed methane and CO_2 plotted in wind rose format with distribution of observed levels broken up in 30-dgree wind sectors.

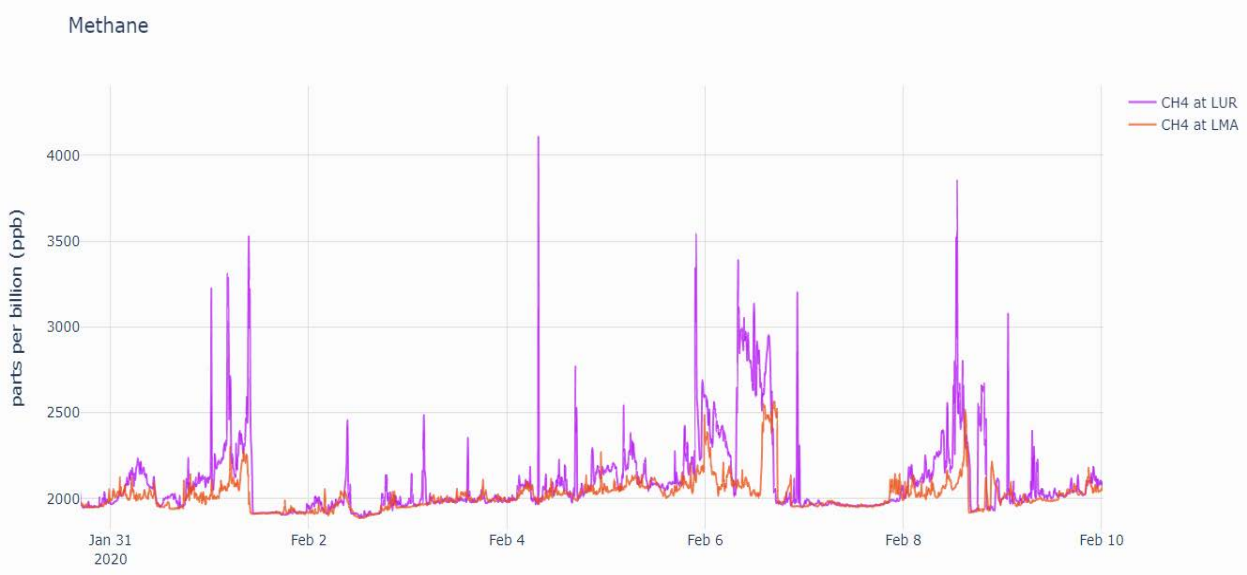

Figure 8:
Concurrent methane observations at LUR and LMA during ten days in February.

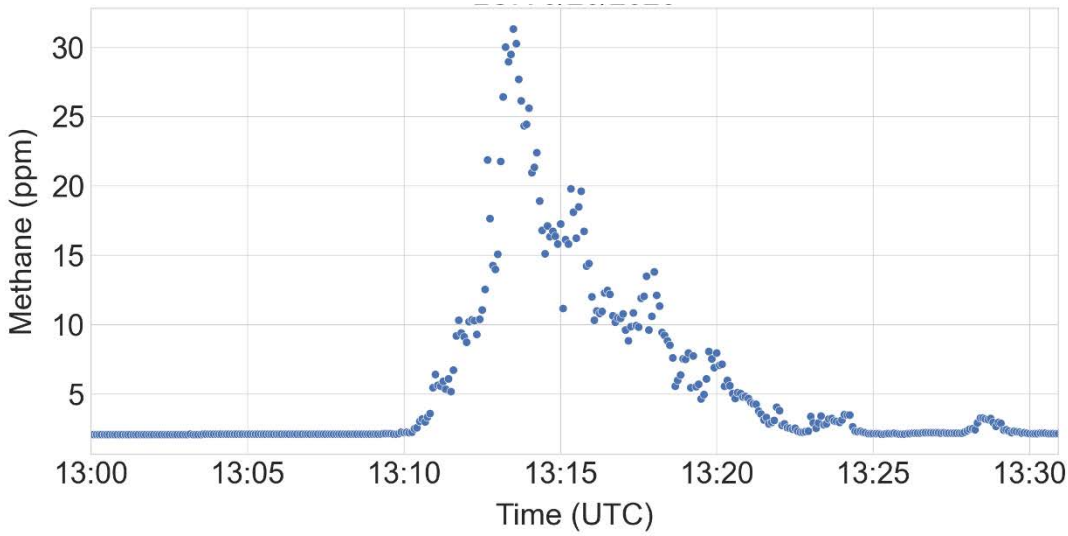

Figure 9:
The highest methane spike observed at LUR on March 26, 2020. This graph uses the high-resolution 5-s data.

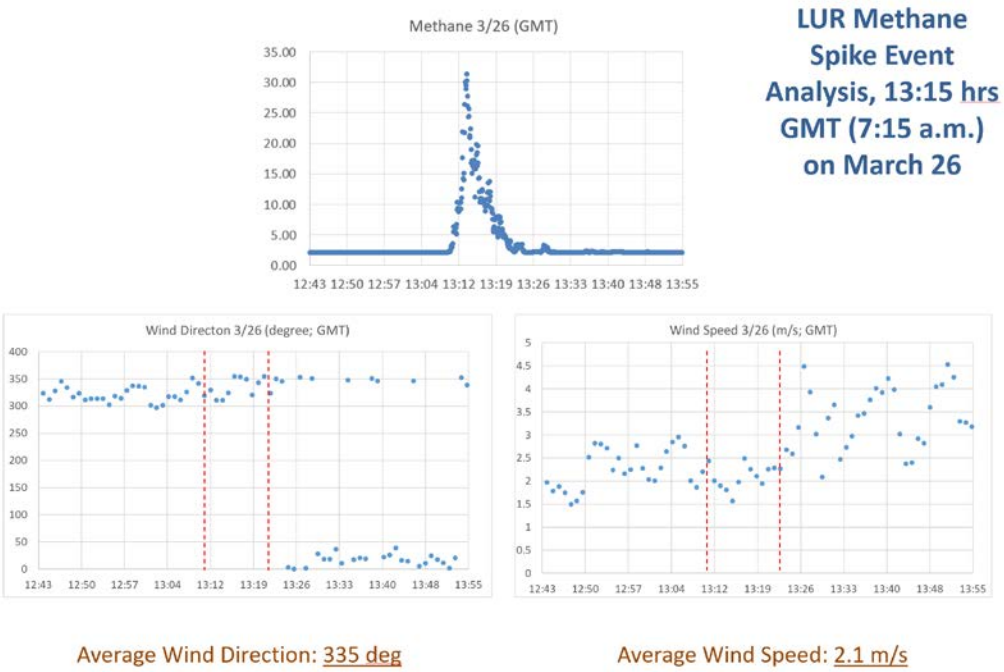

Figure 10:
Wind direction and speed plots during the March 26 methane peak event.

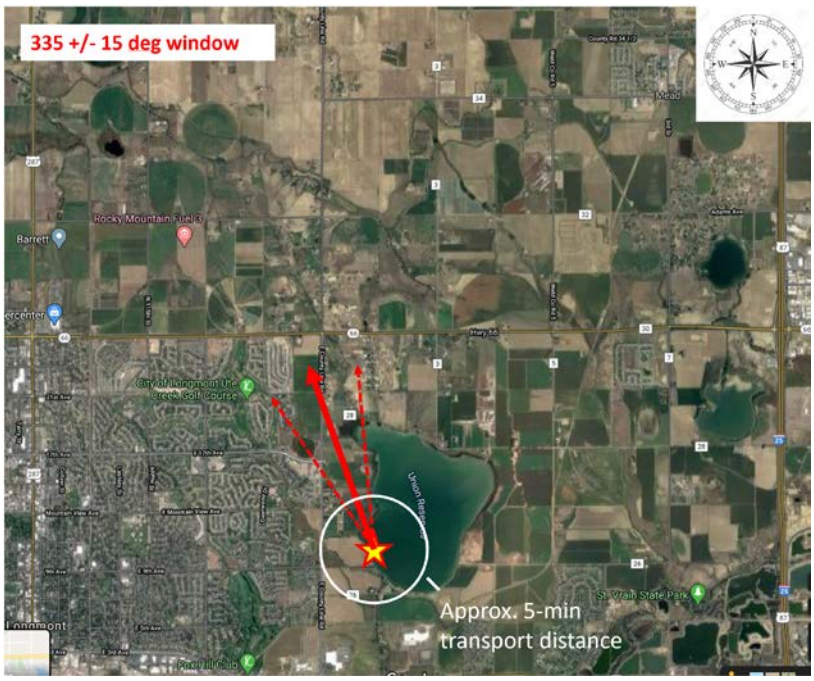

Figure 11:
Wind source direction vector during the March 26, 2020, methane spike, and approximate air transport radius based on observed surface wind speed.

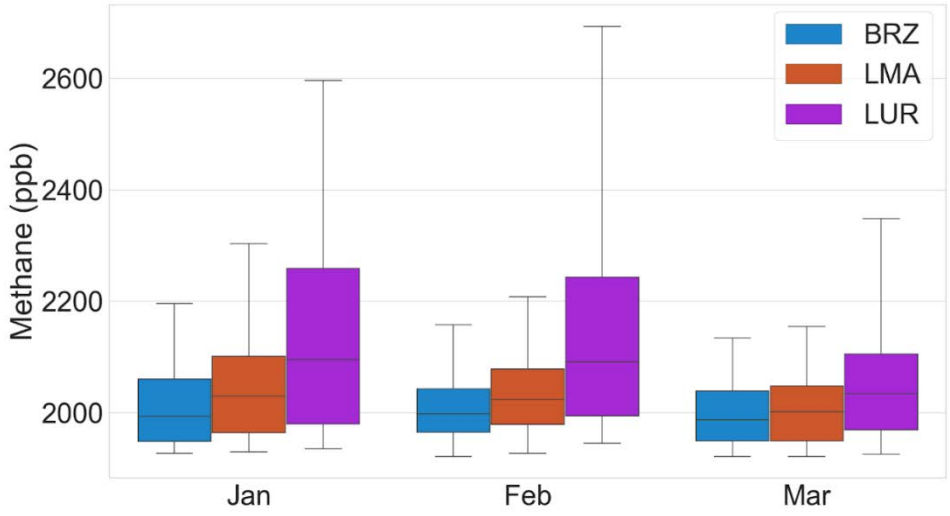

Figure 12:
Comparison of methane distribution at BRZ, LMA, and LUR during Q1, 2020.

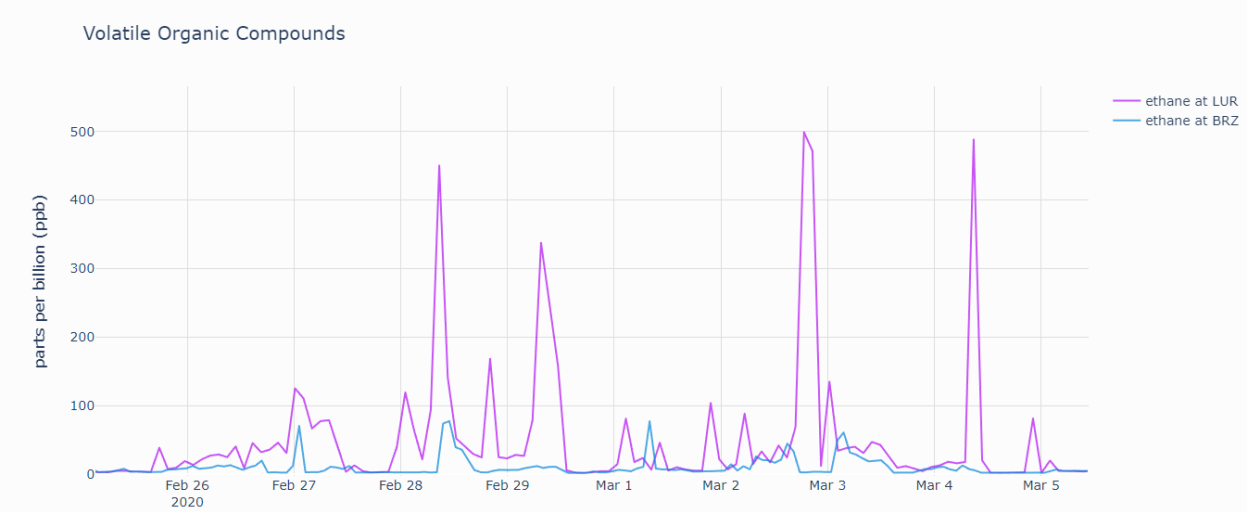

Figure 13:
Ethane distribution at LUR and BRZ during ten days in February-March 2020.

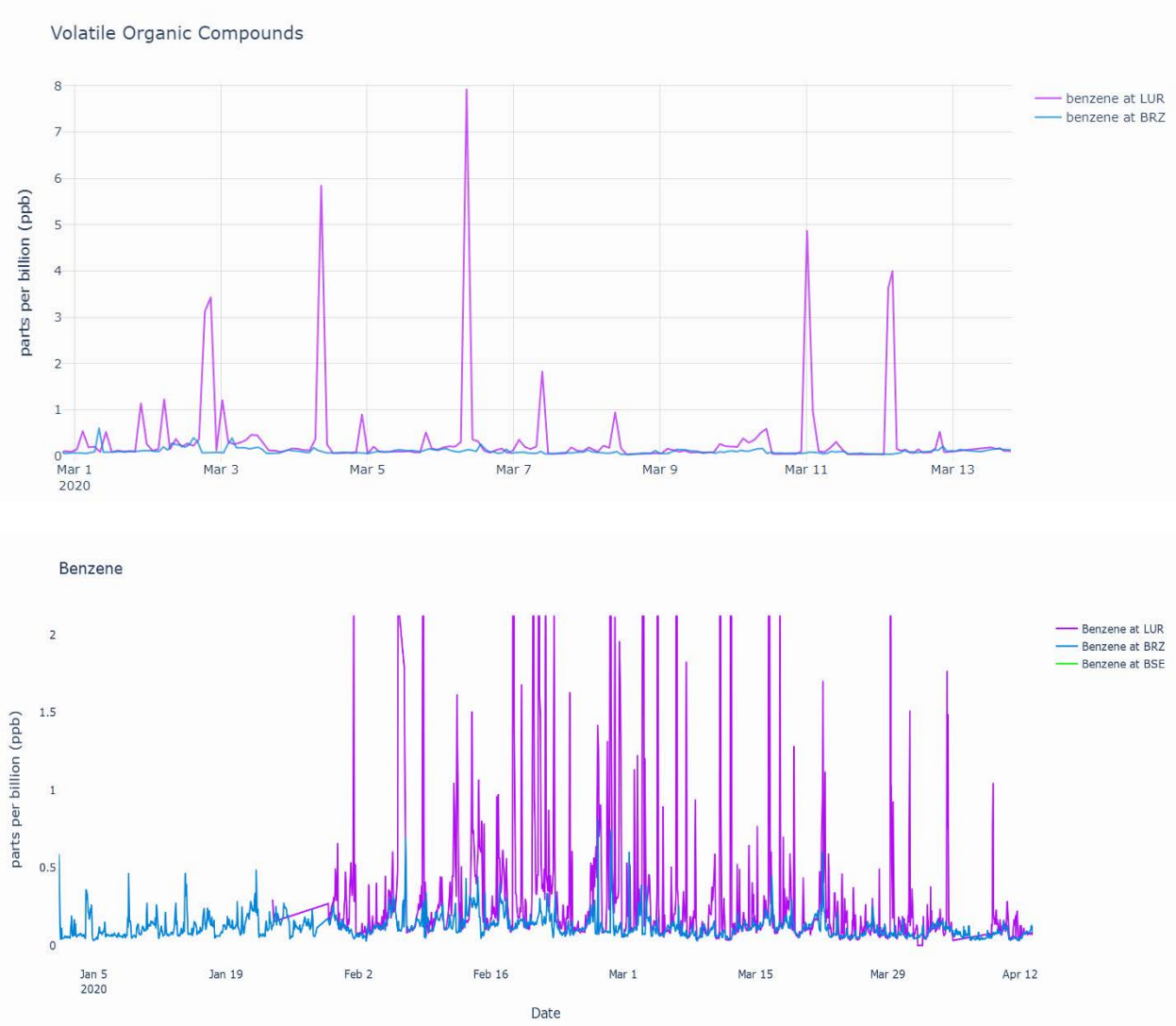

Figure 14:
Comparison of benzene recorded at BRZ and LUR. The upper graph shows an enlargement of the overall record that is plotted in the bottom graph. Please note that the bottom graph y-axis scale maxes out at 2 ppb.

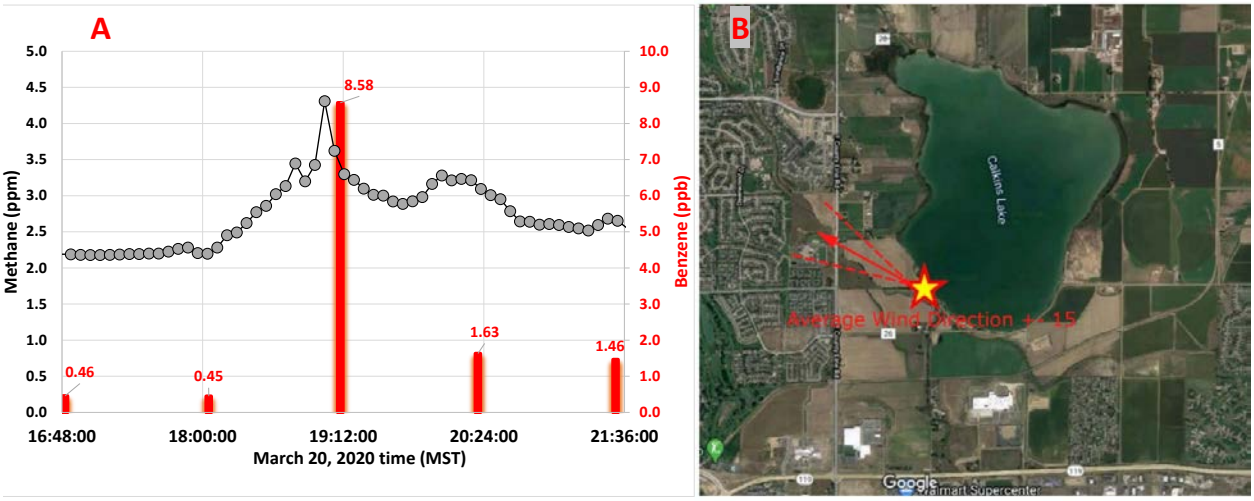

Figure 15:
The maximum benzene observation at LUR during Q1 2020 occurred on March 20 at ~19:00 MST. Panel A shows the 5 individual benzene observations at that time of day along with the co-located methane measurements. In the hours surrounding this event, the wind direction was consistent with low wind speed of ~ 1 m s^{-1}. Panel B shows the wind sector suggesting that the source region was from the west-northwest direction.

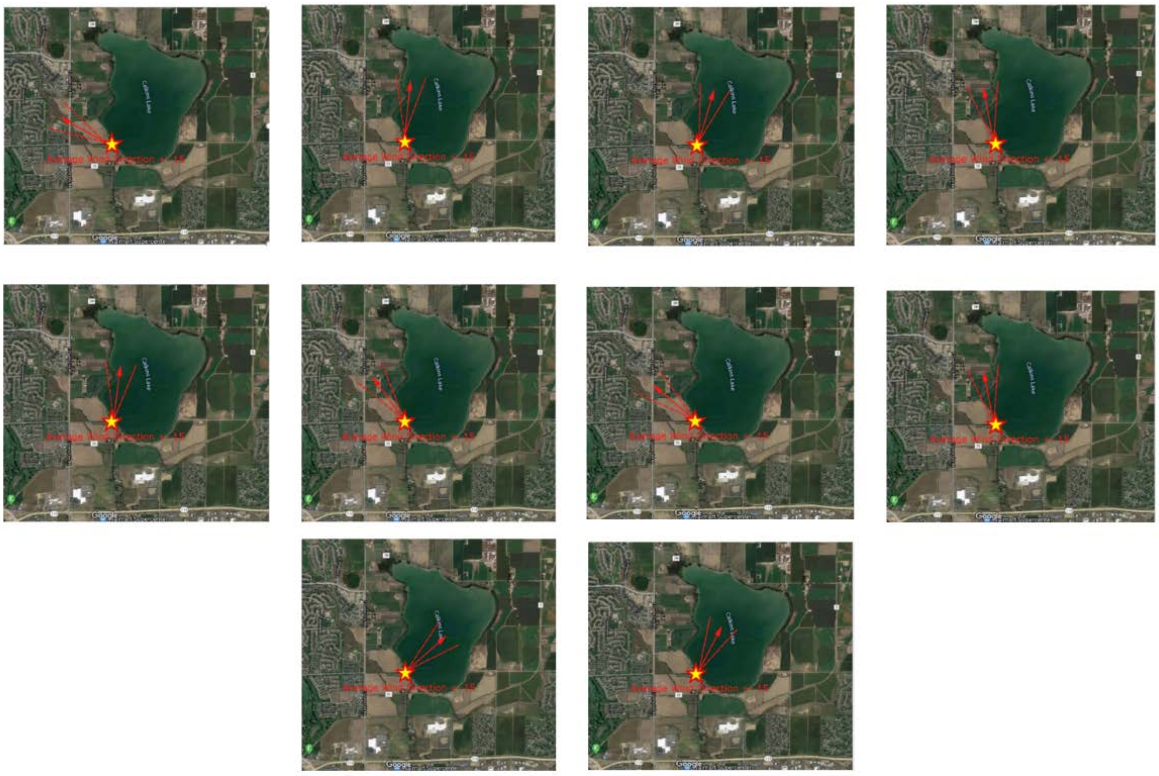

Figure 16:
Wind direction during the ten largest benzene peaks (~4-8 ppb) from January-March. The peaks vary in mixing ratio from around 4 to 8 ppb and in direction from northwest to northeast.

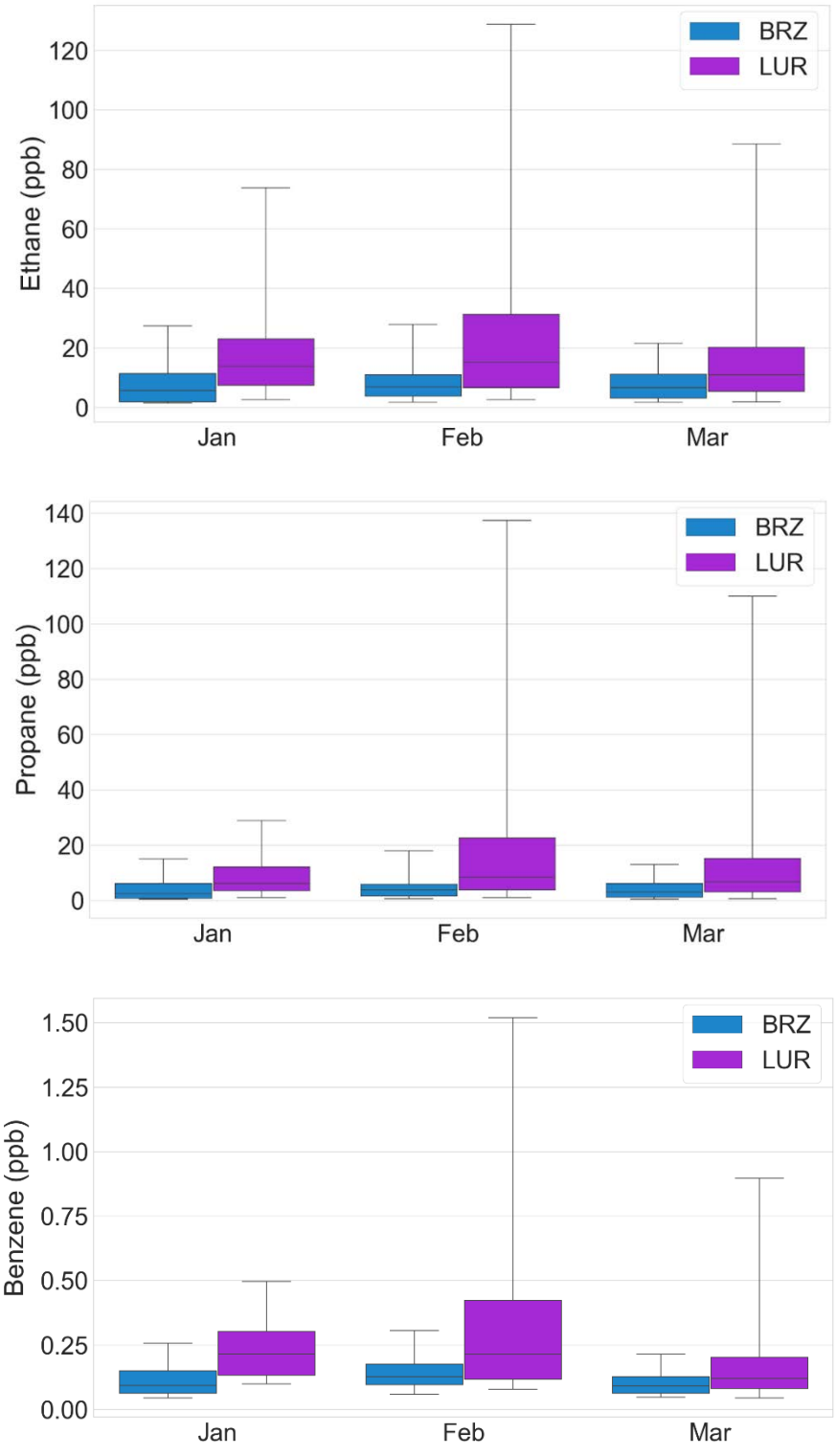

Figure 17:
Comparison of the distribution of ethane, propane, and benzene at BRZ and LUR during Q1. Please note that the LUR VOCs box whisker analyses for January only include three days of data (January 29-31).

Supplement A

Preliminary Data from Longmont Municipal Airport (LMA) during Quarter 1, 2020

Figure SA1:
LMA temperature record January 1 – March 31, 2020.

Figure SA2:
LMA humidity record January 1 – March 31, 2020.

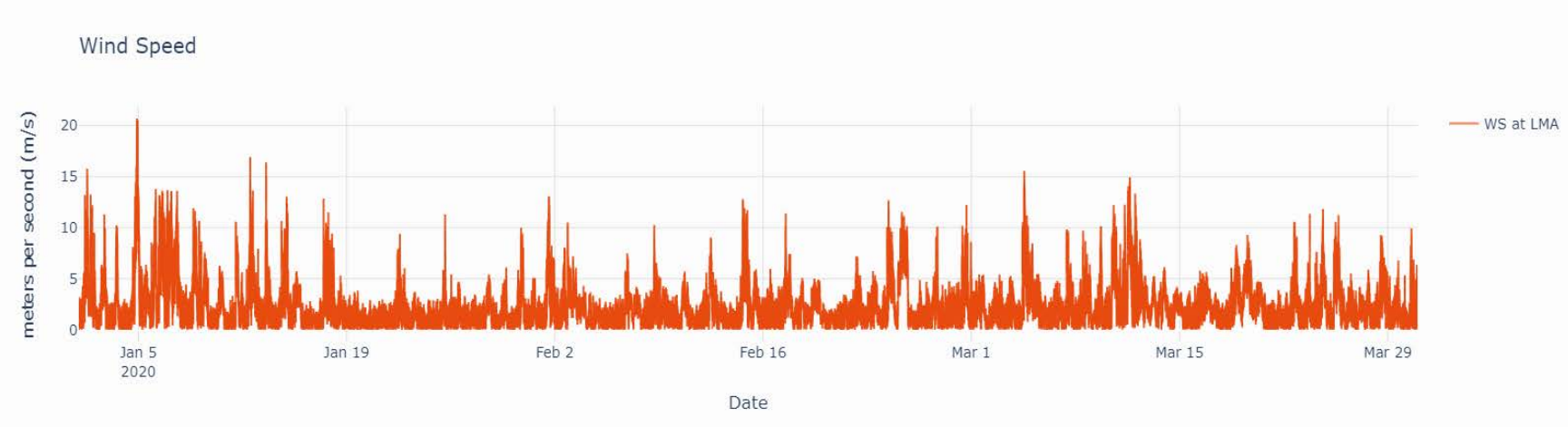

Figure SA3:
LMA wind speed record January 1 – March 31, 2020.

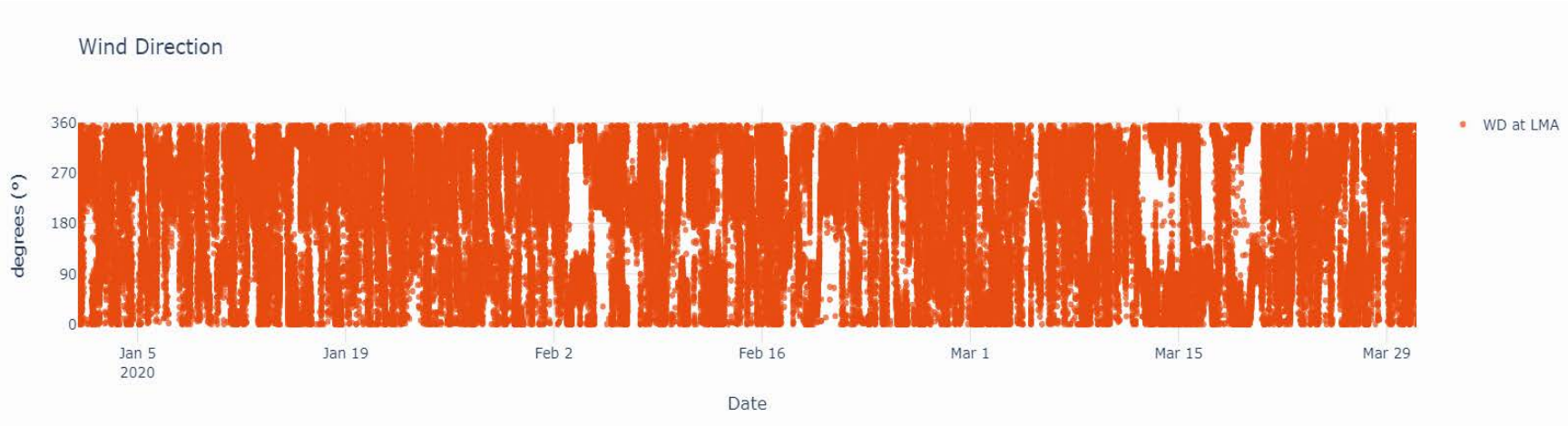

Figure SA4:
LMA wind direction observations: January 1 – March 31, 2020. The resolution of the plot prevents wind direction on individual days to be determined. The complete record is included here to show the completeness of data coverage and to demonstrate the wind direction.

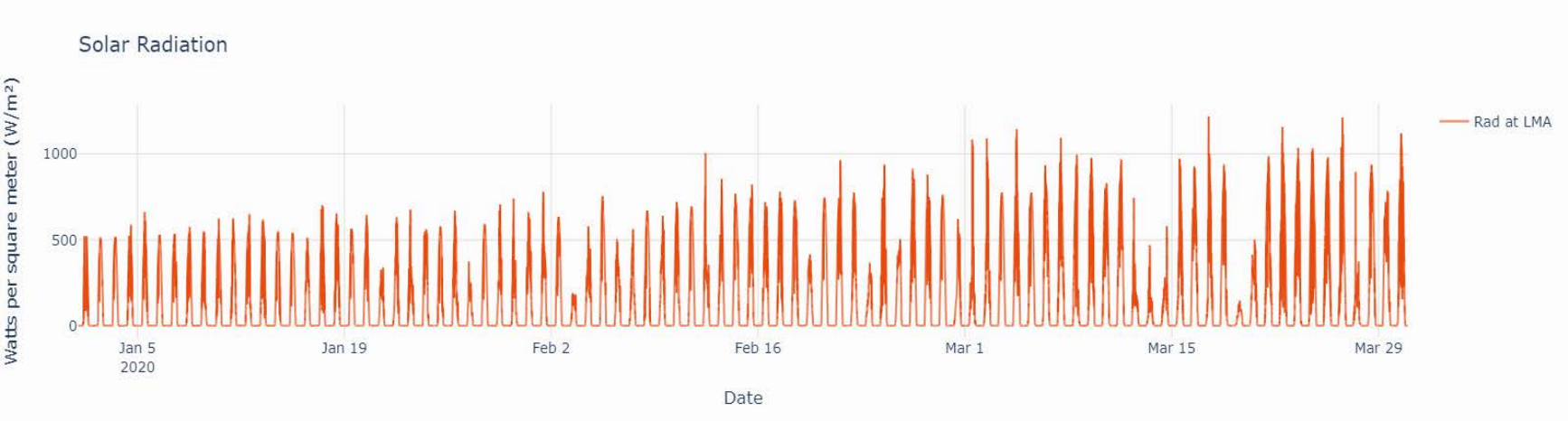

Figure SA5:
LMA solar radiation record January 1 – March 31, 2020.

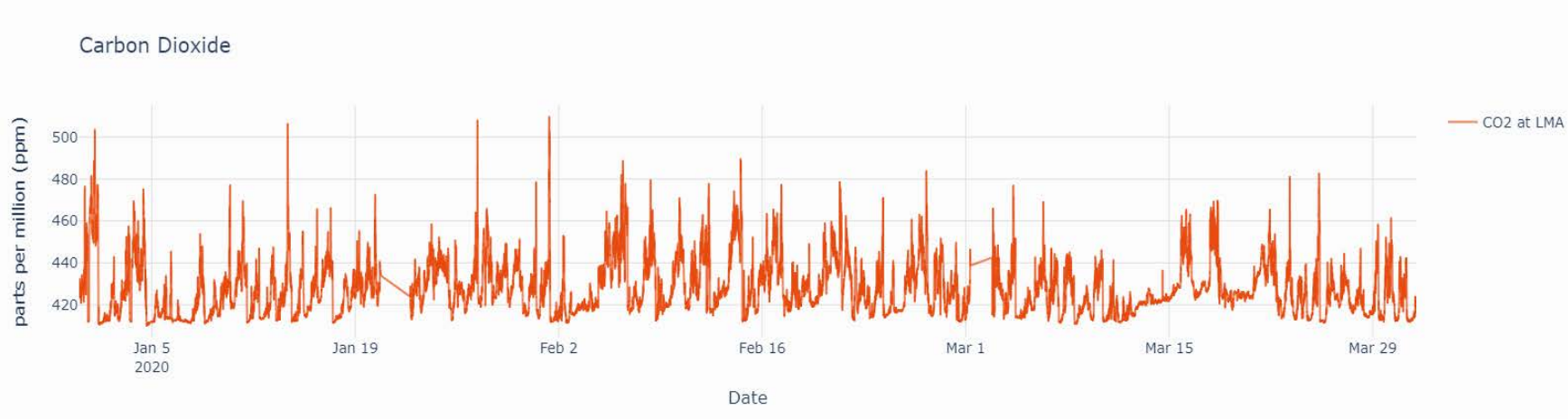

Figure SA6:
LMA CO_2 record January 1 – March 31, 2020.

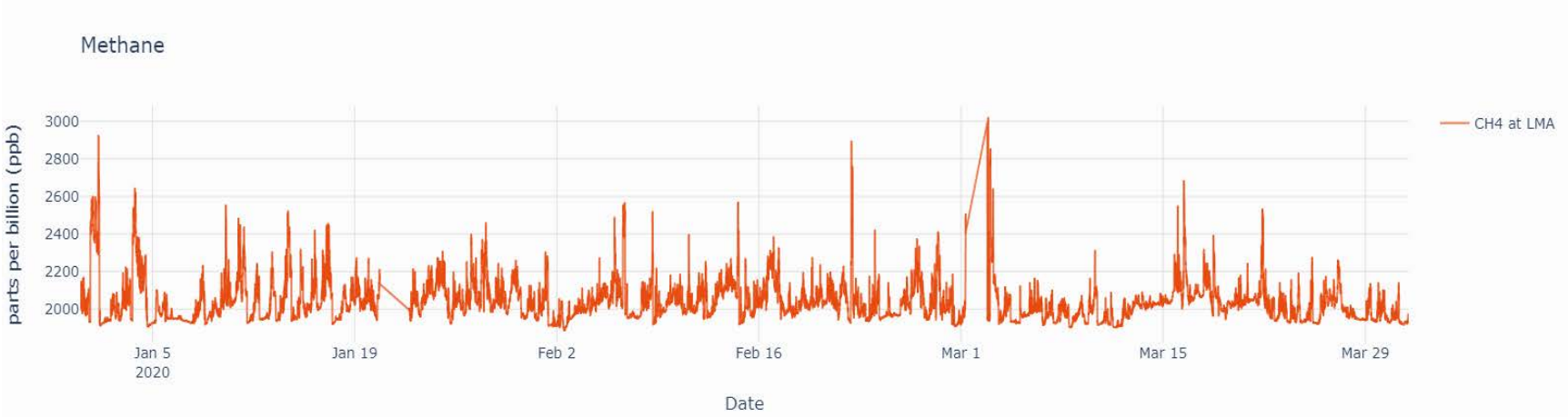

Figure SA7:
LMA methane record January 1 – March 31, 2020.

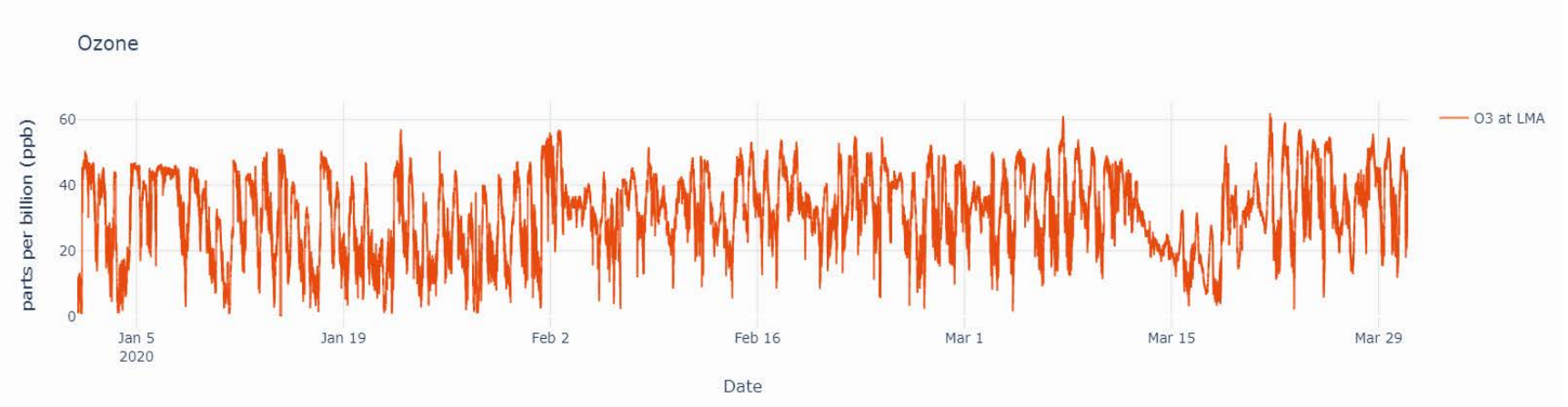

Figure SA8:
LMA ozone record January 1 – March 31, 2020.

Figure SA9:
LMA ozone 8-hour running average record January 1 – March 31, 2020. The yellow line at 70 ppb indicates the NAAQS standard.

Supplement B

Preliminary Data from Longmont Union Reservoir (LUR) 2020

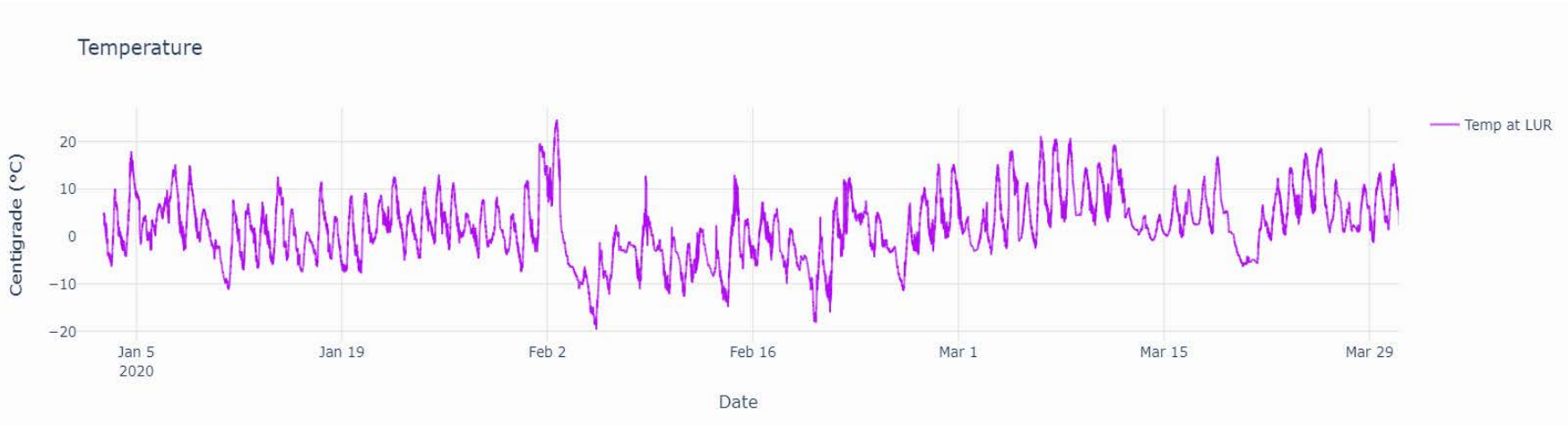

Figure SB1:
LUR temperature record January 1 – March 31, 2020.

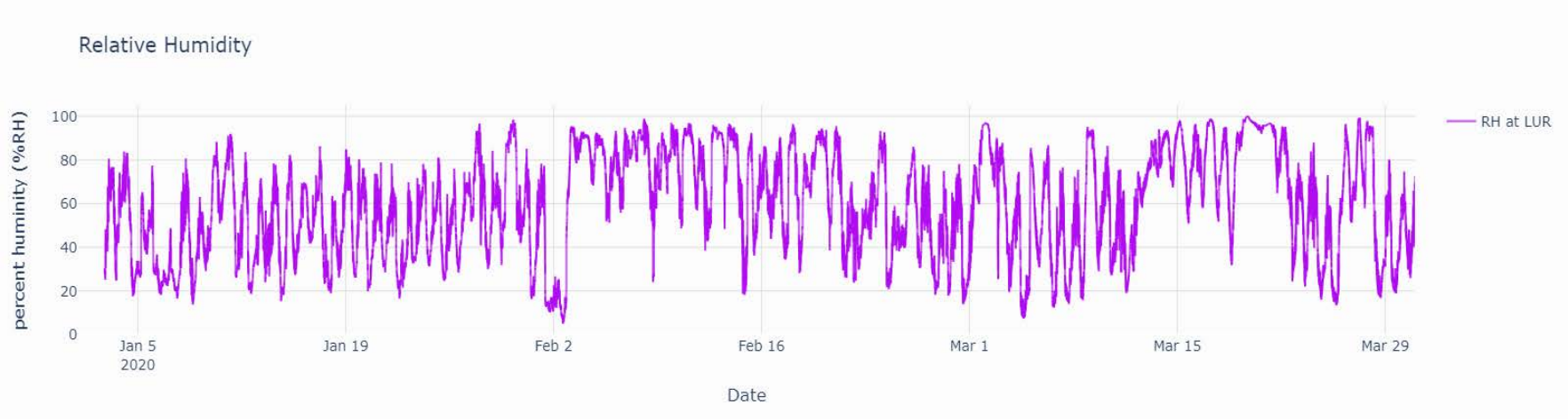

Figure SB2:
LUR humidity record January 1 – March 31, 2020.

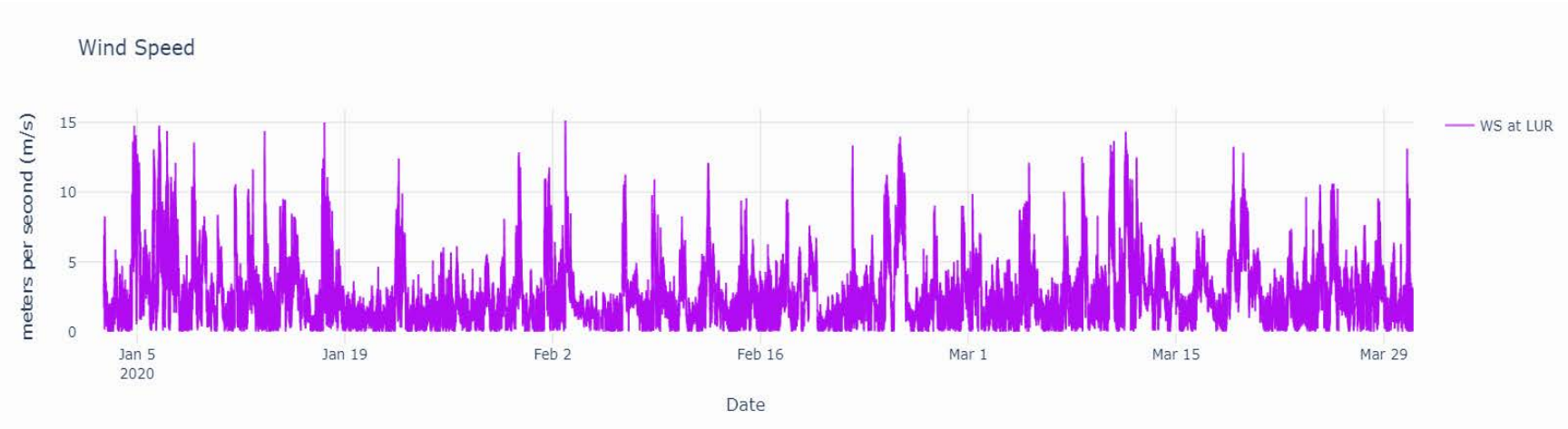

Figure SB3:
LUR wind speed record January 1 – March 31, 2020.

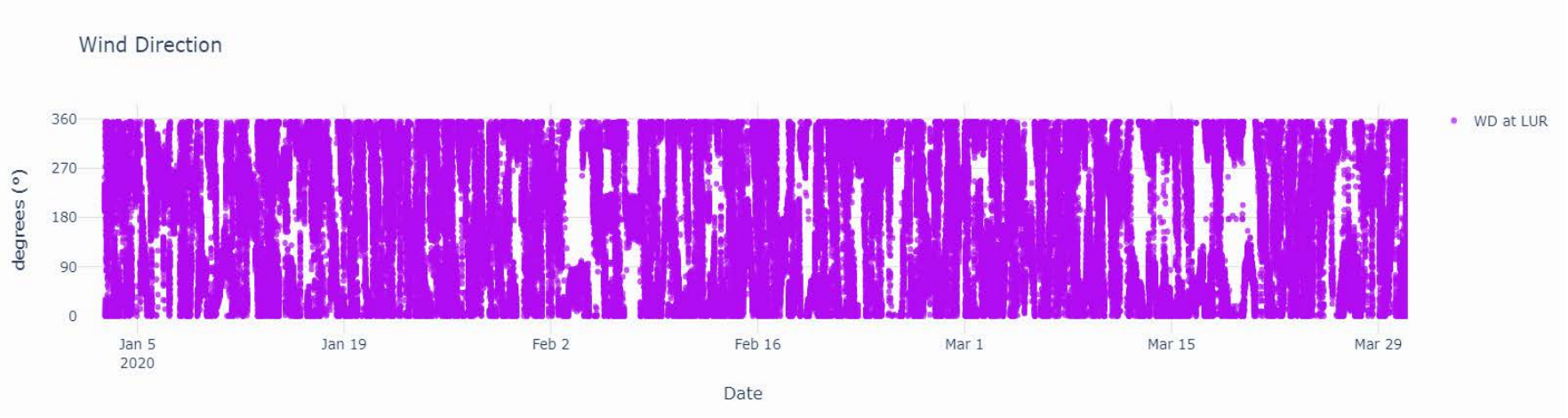

Figure SB4:
LUR wind direction observations: January 1 – March 31, 2020. The resolution of the plot prevents wind direction on individual days to be determined. The complete record is included here to show the completeness of data coverage and to demonstrate the wind direction.

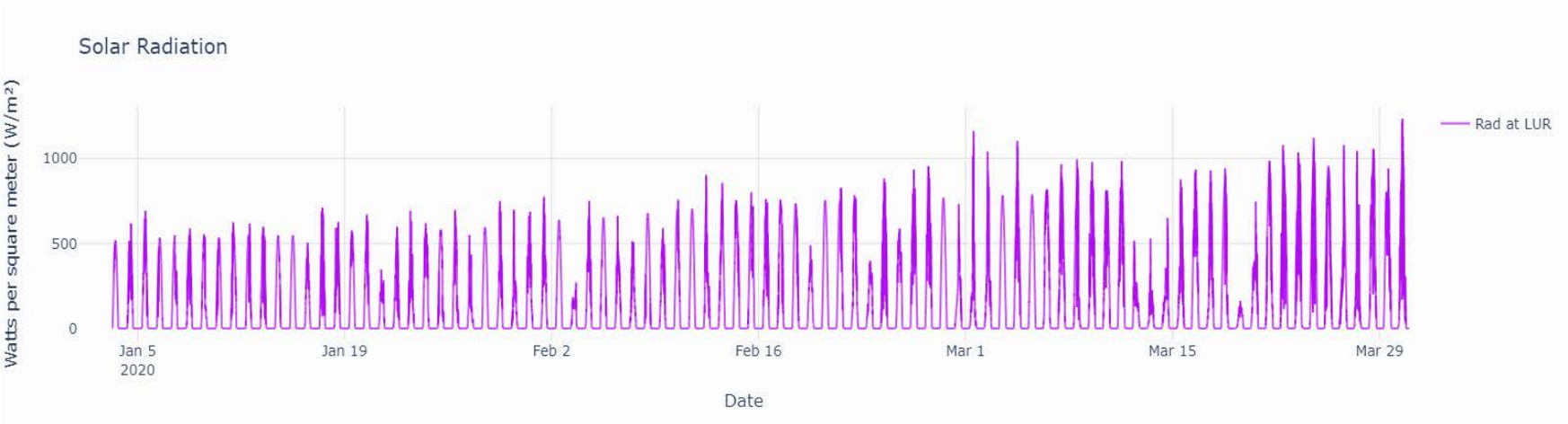

Figure SB5:
LUR solar radiation record January 1 – March 31, 2020.

Figure SB6:
LUR CO_2 record January 1 – March 31, 2020.

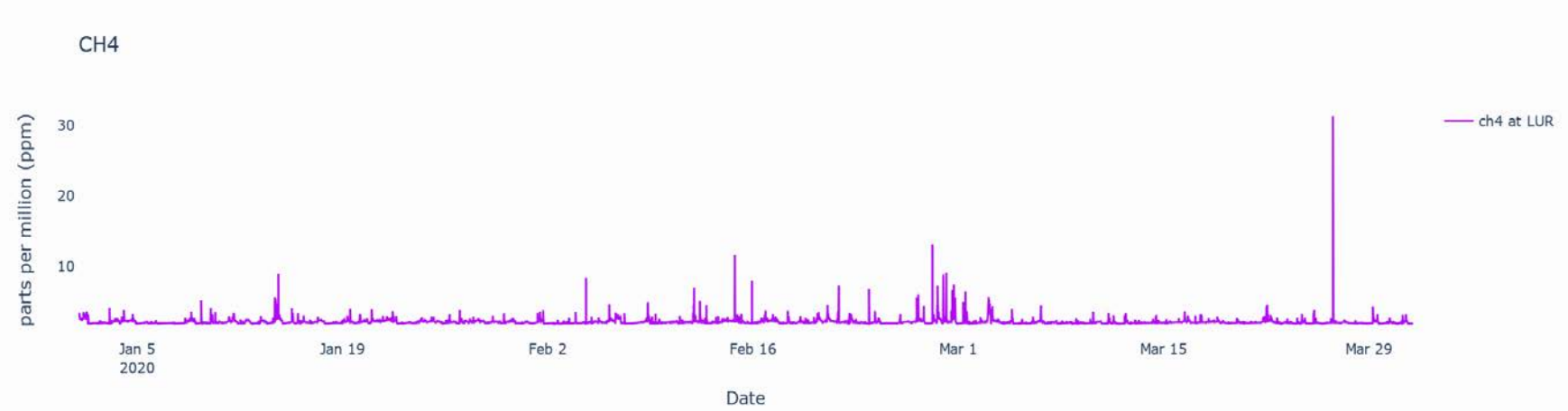

Figure SB7:
LUR methane record January 1 – March 31, 2020.

Figure SB8:
LUR ozone record January 1 – March 31, 2020.

Figure SB9:
LUR ozone 8-hour running average record January 1 – March 31, 2020. The yellow line at 70 ppb indicates the NAAQS standard.

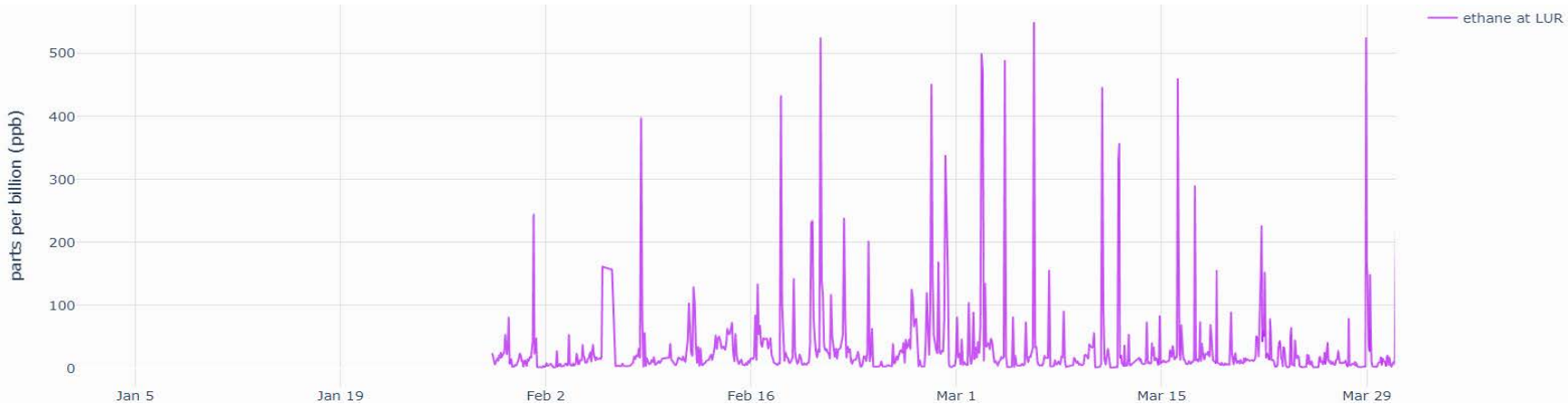

Figure SB10:
LUR ethane record January 1 – March 31, 2020.

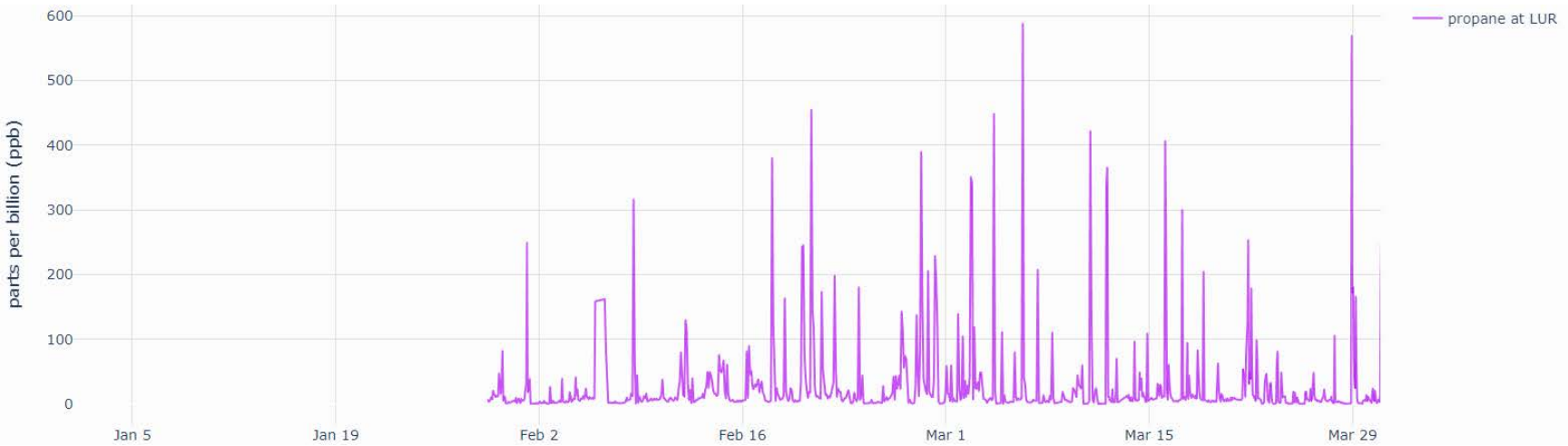

Figure SB11:
LUR propane record January 1 – March 31, 2020.

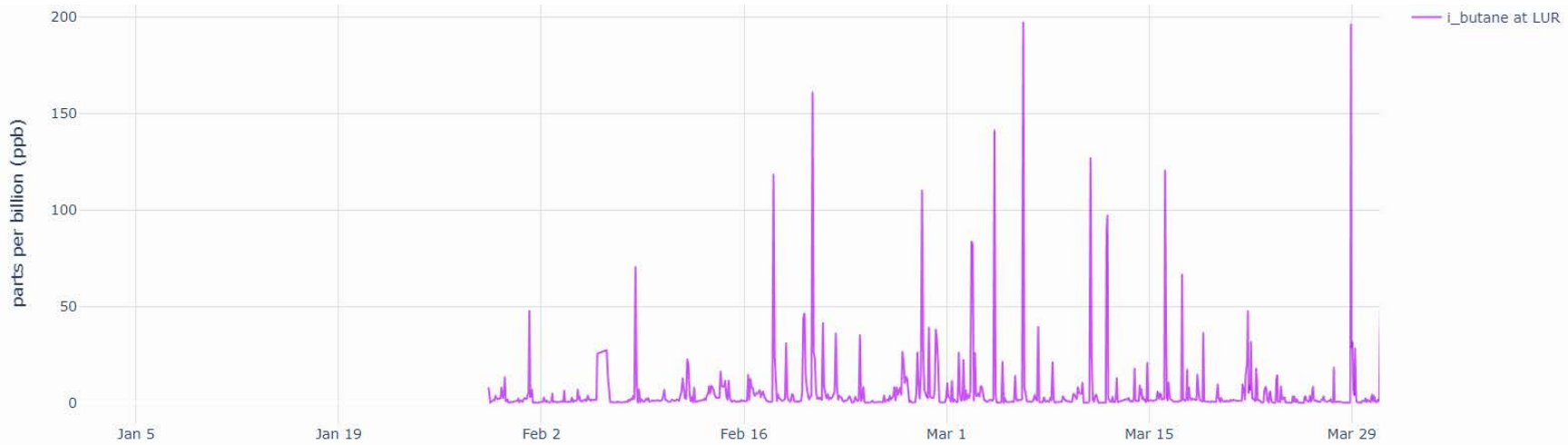

Figure SB12:
LUR i-butane record January 1 – March 31, 2020.

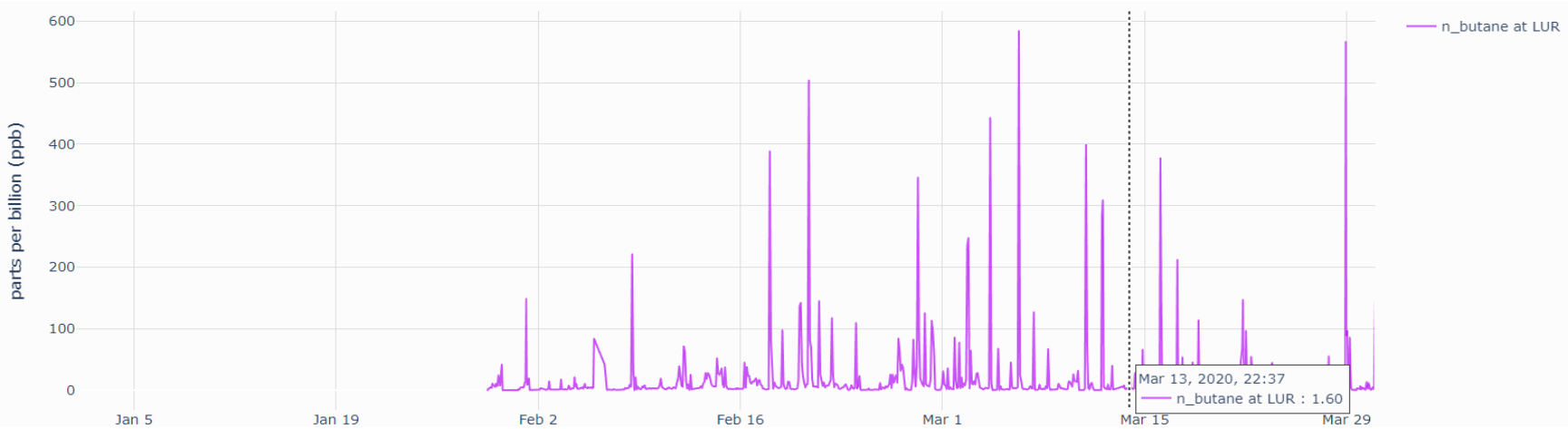

Figure SB13:
LUR n-butane record January 1 – March 31, 2020.

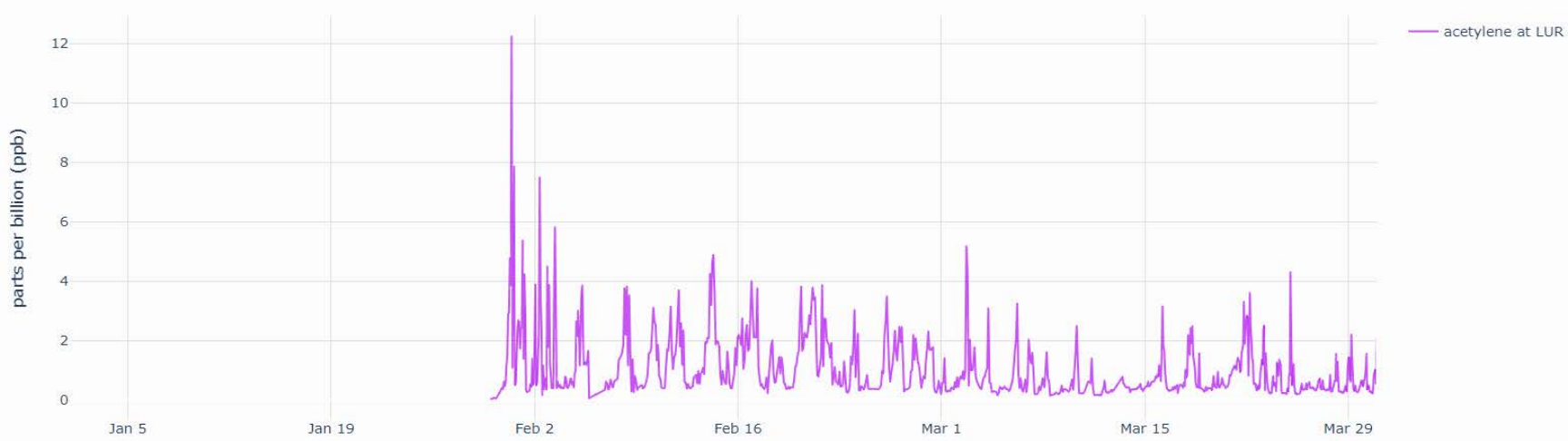

Figure SB14:
LUR acetylene record January 1 – March 31, 2020.

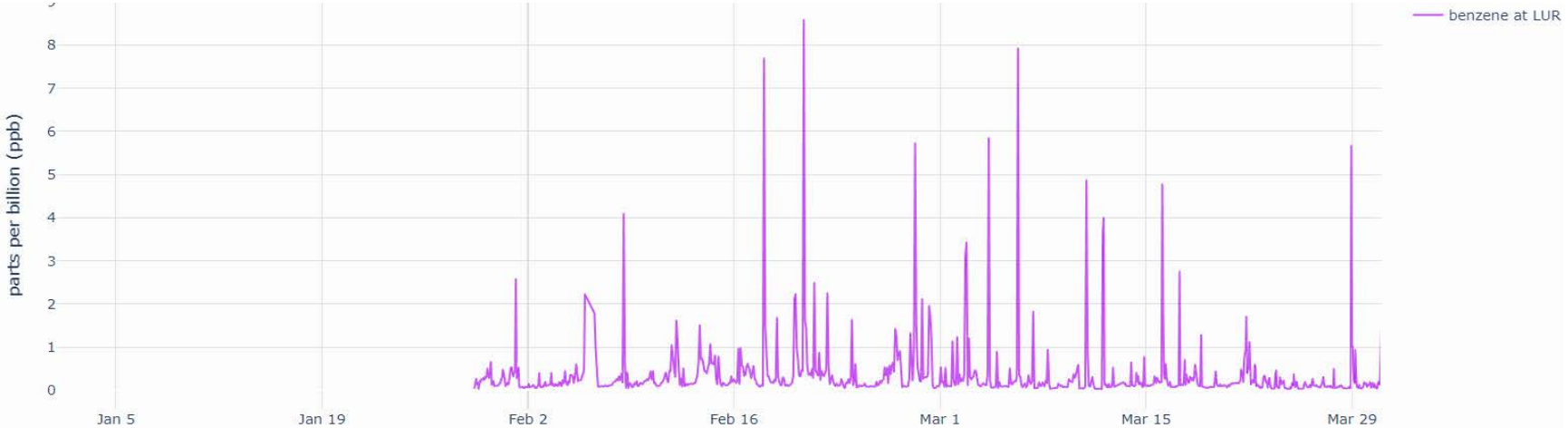

Figure SB15:
LUR benzene record January 1 – March 31, 2020.

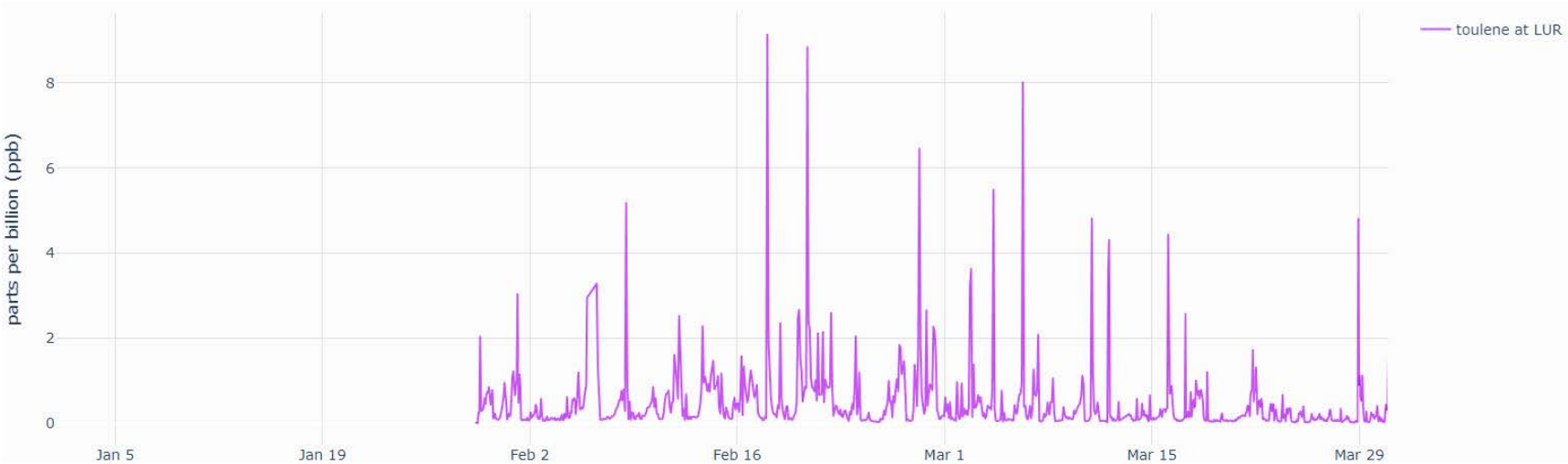

Figure SB16:
LUR toluene record January 1 – March 31, 2020.

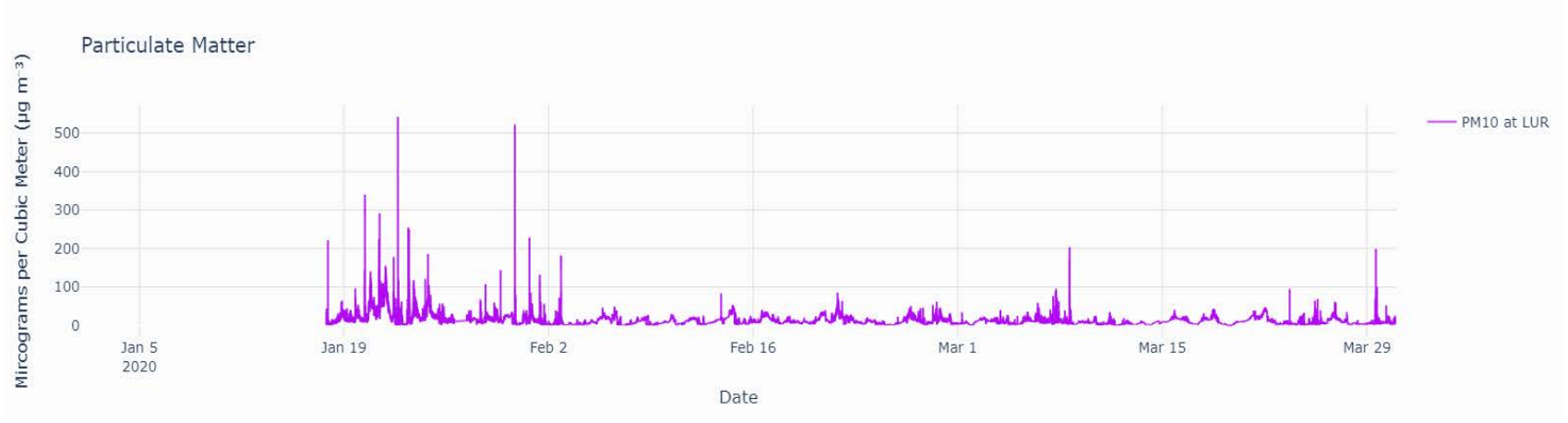

Figure SB17:
LUR 10-hour particulate matter record January 1 – March 31, 2020.

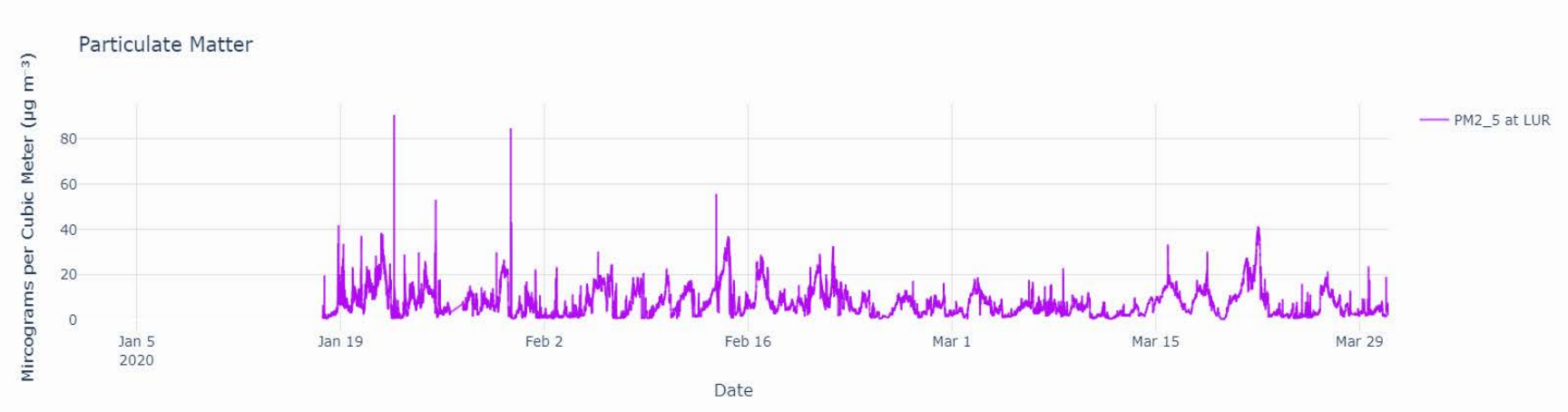

Figure SB18:
LUR 2.5-hour particulate matter record January 1 – March 31, 2020.

Supplement C

Comparison Preliminary Data LMA & LUR during Quarter 1, 2020

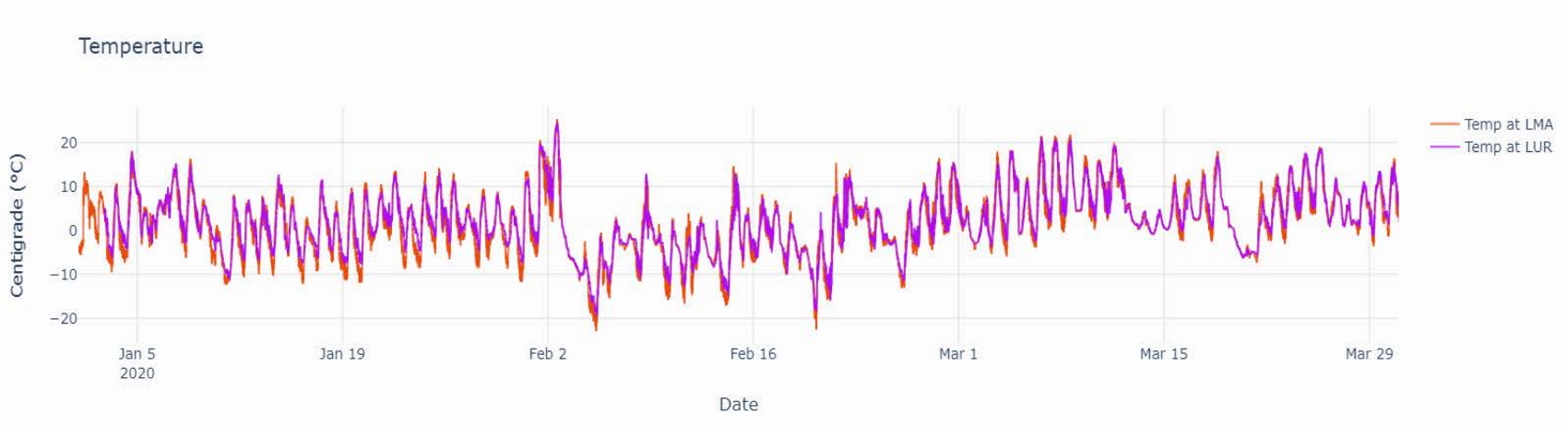

Figure SC1:
LMA & LUR Temperature record January 1 – March 31, 2020.

Figure SC2:
LMA & LUR relative humidity record September January 1 – March 31, 2020.

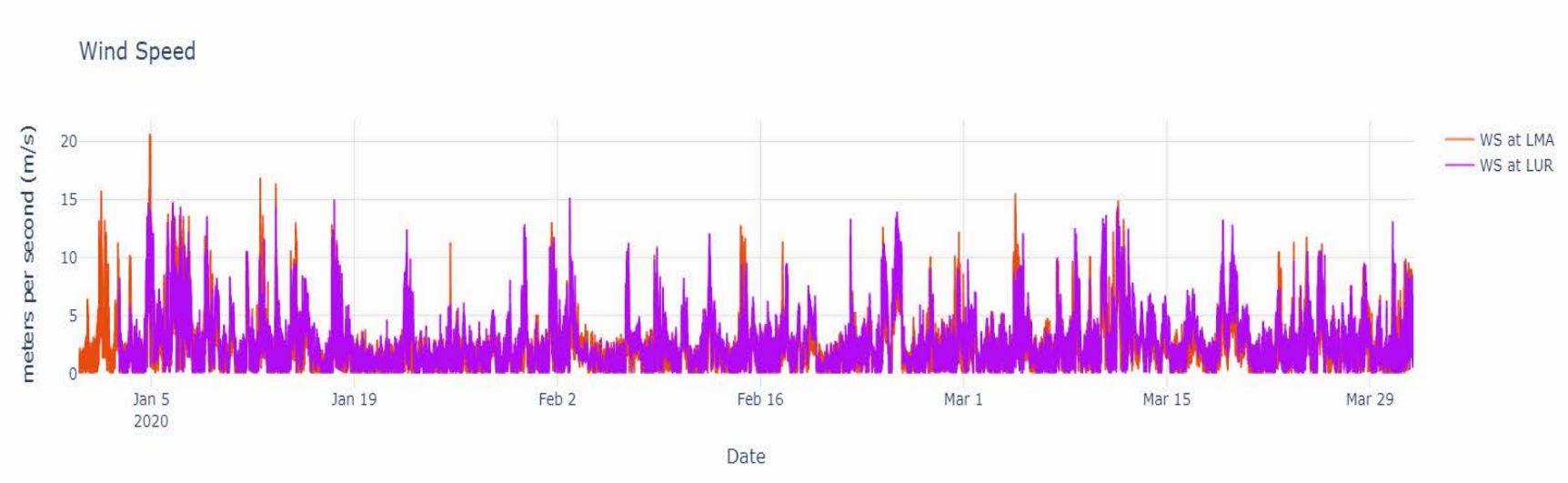

Figure SC3:
LMA & LUR wind speed record January 1 – March 31, 2020.

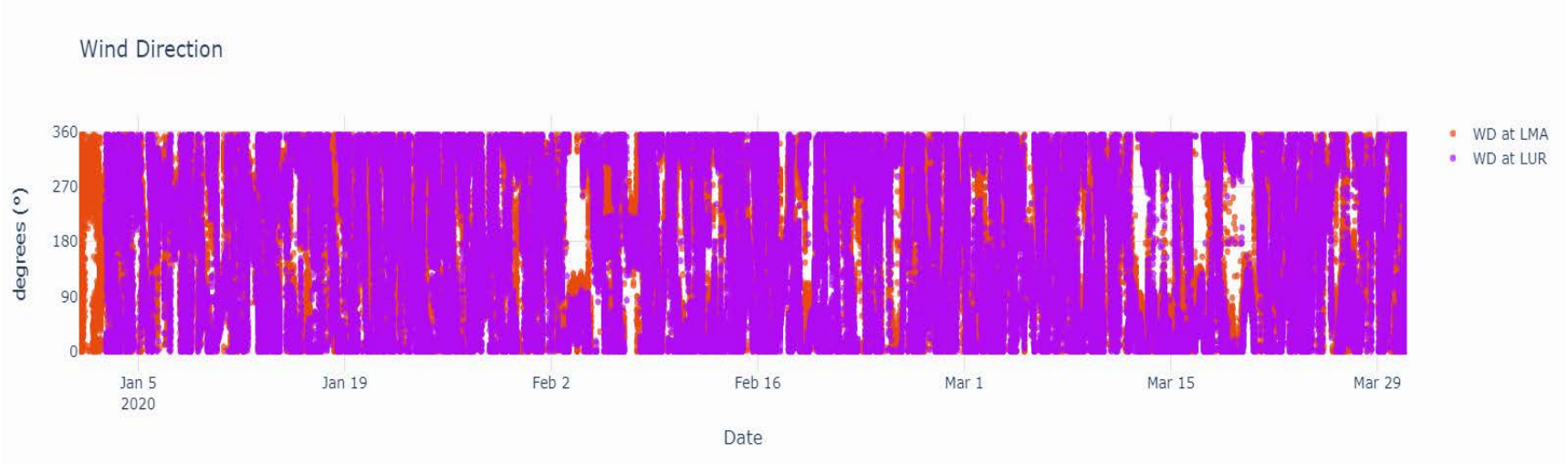

Figure SC4:
LMA & LUR wind direction record January 1 – March 31, 2020.

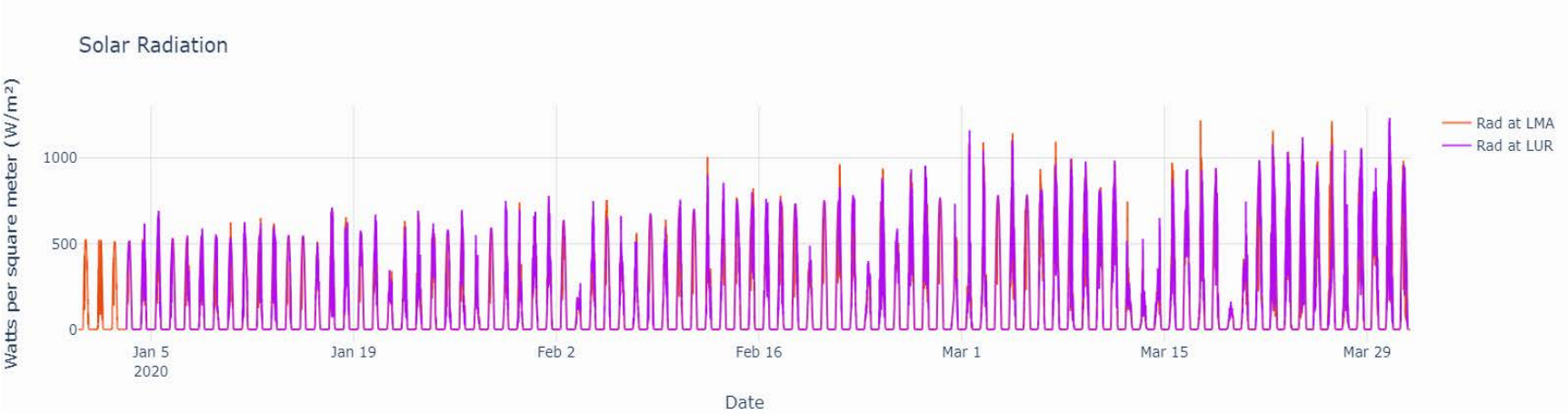

Figure SC5:
LMA & LUR solar radiation record September January 1 – March 31, 2020.

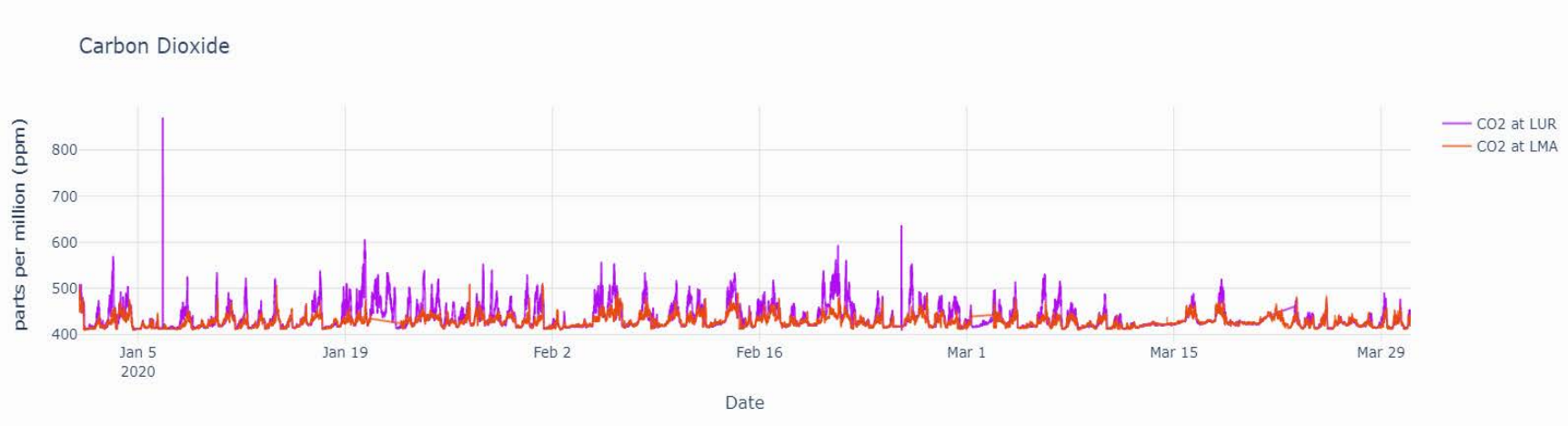

Figure SC6:
LMA & LUR CO_2 record September January 1 – March 31, 2020.

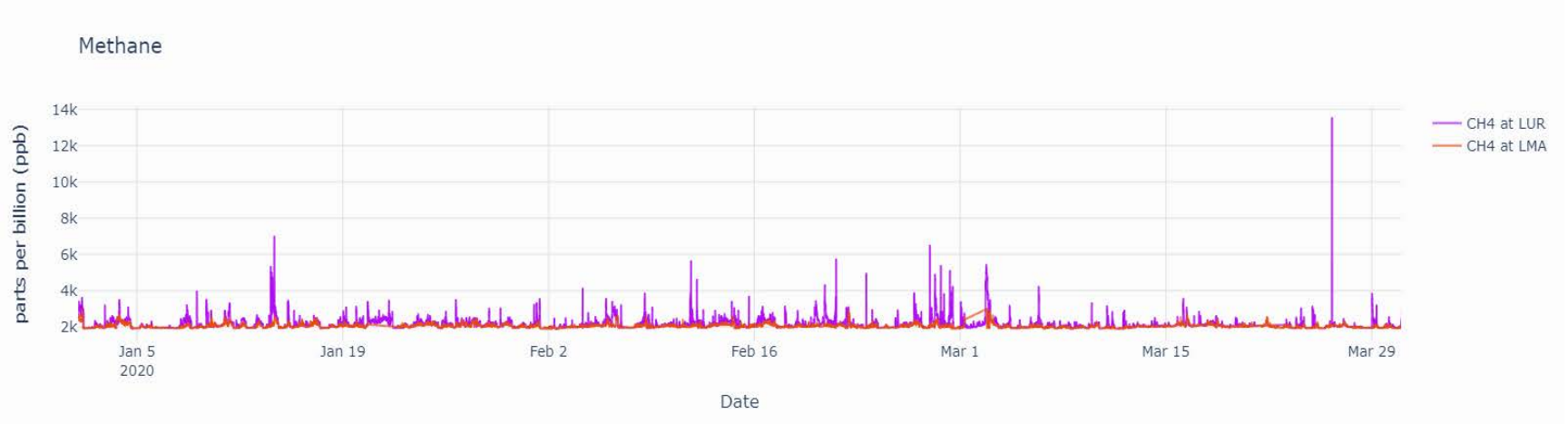

Figure SC7:
LMA & LUR methane record September January 1 – March 31, 2020.

Figure SC7:
LMA & LUR ozone record September January 1 – March 31, 2020.